nature

https://doi.org/10.1038/s41586-024-07849-4

Accelerated Article Preview

Spillover of highly pathogenic avian influenza H5N1 virus to dairy cattle

Received: 22 May 2024

Accepted: 18 July 2024

Accelerated Article Preview

Cite this article as: Caserta, L. C. et al. Spillover of highly pathogenic avian influenza H5N1 virus to dairy cattle. *Nature* https://doi.org/10.1038/s41586-024-07849-4 (2024)

Leonardo C. Caserta, Elisha A. Frye, Salman L. Butt, Melissa Laverack, Mohammed Nooruzzaman, Lina M. Covaleda, Alexis C. Thompson, Melanie Prarat Koscielny, Brittany Cronk, Ashley Johnson, Katie Kleinhenz, Erin E. Edwards, Gabriel Gomez, Gavin Hitchener, Mathias Martins, Darrell R. Kapczynski, David L. Suarez, Ellen Ruth Alexander Morris, Terry Hensley, John S. Beeby, Manigandan Lejeune, Amy K. Swinford, François Elvinger, Kiril M. Dimitrov & Diego G. Diel

Spillover of highly pathogenic avian influenza H5N1 virus to dairy cattle

Leonardo C. Caserta[1#], Elisha A. Frye[1#], Salman L. Butt[1#], Melissa Laverack[1], Mohammed Nooruzzaman[1], Lina M. Covaleda[1], Alexis C. Thompson[2], Melanie Prarat Koscielny[4], Brittany Cronk[1], Ashley Johnson[4], Katie Kleinhenz[2], Erin E. Edwards[3], Gabriel Gomez[3], Gavin Hitchener[1], Mathias Martins[3], Darrell R. Kapczynski[5], David L. Suarez[5], Ellen Ruth Alexander Morris[3], Terry Hensley[3], John S. Beeby[1], Manigandan Lejeune[1], Amy K. Swinford[3], François Elvinger[1], Kiril M. Dimitrov[3*], & Diego G. Diel[1*]

[1]Department of Population Medicine and Diagnostic Sciences, Animal Health Diagnostic Center, College of Veterinary Medicine, Cornell University, Ithaca, NY, USA.

[2]Texas A&M Veterinary Medical Diagnostic Laboratory, Canyon, TX, USA.

[3]Texas A&M Veterinary Medical Diagnostic Laboratory, College Station, TX, USA.

[4]Ohio Animal Disease and Diagnostic Laboratory, Ohio Department of Agriculture, Reynoldsburg, OH, USA.

[5]Southeast Poultry Research Laboratory, U.S. National Poultry Research Center, Agricultural Research Service, United States Department of Agriculture, Athens, GA, USA.

[#]These authors contributed equally to this work.

[*]Correspondence to: kiril.dimitrov@tvmdl.tamu.edu & dgdiel@cornell.edu.

Summary

Highly pathogenic avian influenza (HPAI) H5N1 clade 2.3.4.4b virus has caused the death of millions of domestic birds and thousands of wild birds in the U.S. since January, 2022[1–4] Throughout this outbreak, spillovers to mammals have been frequently documented[5–12]. We report spillover of HPAI H5N1 virus in dairy cattle herds across several states in the U.S. The affected cows displayed clinical signs encompassing decreased feed intake, altered fecal consistency, respiratory distress, and decreased milk production with abnormal milk. Infectious virus and viral RNA were consistently detected in milk from affected cows. Viral distribution in tissues via immunohistochemistry and *in situ* hybridization revealed a distinct tropism of the virus for the epithelial cells lining the alveoli of the mammary gland in cows. Whole viral genome sequences recovered from dairy cows, birds, domestic cats, and a raccoon from affected farms indicated multidirectional interspecies transmissions. Epidemiologic and genomic data revealed efficient cow-to-cow transmission after apparently healthy cows from an affected farm were transported to a premise in a different state. These results demonstrate the transmission of HPAI H5N1 clade 2.3.4.4b virus at a non-traditional interface underscoring the ability of the virus to cross species barriers.

46 **Main**

47 The highly pathogenic avian influenza (HPAI) virus H5Nx goose/Guangdong lineage, an
48 influenza A virus (IAV) from the family *Orthomyxoviridae*, emerged in China in 1996. This viral
49 lineage was initially detected only in poultry with detections in wild birds occurring in 2002[13].
50 The virus has frequently reassorted with other influenza viruses, with the hemagglutinin gene
51 remaining as the only gene that defines this genetic lineage of viruses. These frequent
52 reassortments and ongoing antigenic changes required complex classification into multiple
53 clades[14]. Over the past decade, H5Nx goose/Guangdong lineage evolved into eight clades
54 (2.3.4.4a-2.3.4.4h) with three main neuraminidase subtypes: N1, N8 and N6. The H5N1 clade
55 2.3.4.4b has caused global outbreaks in recent years[15,16], infecting various avian species and
56 showing potential to infect humans and other mammals[5,6,22,23,7,11,12,17–21]. The World Health
57 Organization (WHO) reports 860 human infections since 2003, with a fatality rate of
58 approximately 52.8%[24], although serologic evidence suggests less severe more widespread
59 infection[25]. Risk of human-to-human transmission remains low[26]. Since 2016, H5Nx clade
60 2.3.3.4b has circulated broadly in migratory wild bird populations across Europe, Africa, and Asia,
61 being first detected in North America (Canada) in December 2021[27]. By January 2022, it was
62 found in wild birds in North and South Carolina in the U.S.[28,1], and soon after in commercial
63 poultry[2]. Since then, H5N1 caused high morbidity and mortality in poultry leading to the loss of
64 over 90 million birds in the U.S. alone[29] The continuous and widespread circulation of this high-
65 consequence panzootic pathogen in the U.S. is of major concern and poses a significant threat to
66 animal and public health.

67 In addition to devastating consequences to domestic and wild avian species, H5N1 clade
68 2.3.4.4b spillovers have been detected in several mammalian species[9,10,30,29], including domestic

69 and wild carnivorous species such as cats (*Felis catus*)[17], red foxes (*Vulpes Vulpes*)[6], bears (*Ursus*
70 *americanus)*[11], and harbor seals (*Phoca vitulina*)[5]. The virus has even spread to polar regions,
71 killing a polar bear (*Ursus maritimus*) in the Arctic and elephant (*Mirounga leonine*) and Antarctic
72 fur (*Arctocephalus gazella*) seals and gentoo penguins (*Pygoscelis papua*) in Antarctica[31]. In the
73 U.S., a human infection in a poultry worker resulted in mild symptoms and full recovery[32]. During
74 2023, two major outbreaks of H5N1 in harbor seals resulted in high mortality in Maine and
75 Washington. In January 2023, two indoor-outdoor cats died from HPAI-induced encephalitis[12].
76 Acute death of a striped skunk (*Mephitis mephitis*) in Washington was reported[20] along with
77 additional cases in this species in 2023 and 2024[33]. On March 20, 2024, the Minnesota board of
78 animal health reported that a juvenile goat (*Capra hircus*) tested positive for HPAI, making the
79 first report of HPAI H5N1 infection in a ruminant species; following positive tests in backyard
80 poultry on the same premises[34].

81 Here we report the spillover of HPAI H5N1 clade 2.3.4.4b virus into dairy cattle and
82 describe the findings of a clinical, pathological, and epidemiological investigation in nine affected
83 farms (Farms 1 to 9) across four states in the U.S.

84 **Clinico-epidemiological investigation**

85 From late January-to-mid-March 2024, a morbidity event of unknown etiology affecting dairy
86 cattle was reported by field veterinarians in the Texas Panhandle and surrounding States (New
87 Mexico [NM] and Kansas [KS]). The first farm known to be affected by the morbidity event
88 (January 30, 2024) was in TX; however, no clinical samples were collected from affected animals
89 in this farm. The disease was subsequently reported in additional farms in TX and other states. We
90 conducted a clinic-epidemiological investigation in nine farms located in TX (Farms 1, 2, 5, 6, and
91 7), NM (Farms 4 and 8), KS (Farm 9) and OH (Farm 3) that reported the morbidity event between

92 February 11 and March 19, 2024. Farm 3 in OH was affected after apparently healthy lactating
93 cattle were transported from Farm 1 in TX to this location (**Extended Data Table 1**). Affected
94 dairy cattle presented with decreased feed intake, decreased rumination time, mild respiratory
95 signs (clear nasal discharge, increased respiratory rate, and labored breathing), lethargy,
96 dehydration, dry/tacky feces or diarrhea, and milk with abnormal yellowish colostrum-like color,
97 thick and sometimes curdled consistency. Additionally, an abrupt drop in milk production ranging
98 from 20-100% in individual affected animals was noted. Upon clinical examination, mammary
99 gland involution was observed in several of the affected cows (**Extended Data Fig. 1**). The
100 proportion of clinically affected animals ranged between 3% and 20%. Mortality above average
101 (2-fold higher) was noted cows in Farms 2 and 3 during the clinical event. Notably, several of the
102 affected farms reported simultaneous mortality events in passerines (great-tailed grackles
103 [*Quiscalus mexicanus*]), peridomestic birds (rock pigeons [*Columbia livia*]), and in outdoor
104 domestic (cats) and wild mammals (raccoons [*Procyon lotor*]) (**Extended Data Table 1**). The
105 clinical disease in dairy cattle lasted 5-14 days, with animals returning to pre-outbreak health
106 status, rumination times, and feed intake, but maintaining decreased milk production for at least
107 four weeks.

108 **Multispecies detection of H5N1 virus**

109 A diagnostic investigation was conducted in samples collected from Farms 1-9. Initially, nasal
110 swabs, serum, and blood buffy coats from 10 affected cows from Farm 1 were subjected to viral
111 metagenomic sequencing. Influenza A (IAV) virus sequences were detected in one nasal swab and
112 no other bovine respiratory viruses were detected. Real-time reverse-transcriptase PCR (rRT-PCR)
113 targeting the IAV matrix (M) and hemagglutinin 5 (H5) genes confirmed the presence of HPAI-
114 H5 in nasal swabs of this cow. Notably, 8 of 10 milk samples collected from the same cows were

115 positive for HPAI-H5 via rRT-PCR (**Supplementary Data Table 1**). Additionally, oropharyngeal
116 swabs from great-tailed grackles and rock pigeons, and lung and brain tissues from a cat found
117 dead on Farm 1 tested positive for HPAI-H5 (**Supplementary Data Table 1**). A similar
118 epidemiological scenario involving mortality events in domestic and wild mammals was observed
119 in Farms 3, 4, 5, and 8. Six domestic cats died in Farm 3 after the disease onset in dairy cows. Cats
120 found dead on Farms 4 and 5 and cats and a raccoon found dead on Farm 8 tested positive for
121 HPAI-H5.

122 Testing of multiple sample types (n=331) collected from cows from Farms 1-9 by rRT-
123 PCR showed sporadic viral RNA detection in nasal swabs (10/47), whole blood (3/25), and serum
124 (1/15), and most frequent detection in milk (129/192). The milk samples consistently had the
125 highest viral RNA loads of the samples tested. (**Fig. 1A; Supplementary Data Table 1**). Results
126 from rRT-PCR on tissues collected from three affected cows revealed the presence of viral RNA
127 in lung, small intestine, supramammary lymph nodes and mammary gland. The highest viral RNA
128 loads were detected in the mammary gland (**Fig. 1B; Supplementary Data Table 1**),
129 corroborating high viral loads detected in milk. Additionally, hemagglutination inhibition antibody
130 testing in paired serum samples collected from animals in Farm 2 (n=20) confirmed H5N1
131 infection in affected dairy cows (**Fig. 1C**).

132 **Infectious virus shedding in dairy cows**

133 Virus isolation and quantification were performed on milk samples from Farms 1, 2, and 3.
134 Infectious HPAI H5N1 virus was isolated from the pellet of pooled milk samples from 10 cows
135 from Farms 1 and 2 (**Fig. 1D-E**). Notably, virus titers in milk from affected animals ranged from
136 $10^{4.0}$ to $10^{8.8}$ 50% tissue culture infectious dose ($TCID_{50}$) per ml (**Fig. 1F**), demonstrating high

137 infectious viral loads in milk from infected animals. Consistent with this, high viral loads ($10^{7.3}$ to
138 $10^{7.8}$ $TCID_{50}.ml^{-1}$) were detected in mammary gland tissues (**Fig. 1G**).

139 Virus shedding was also investigated in samples (milk, nasal swabs, urine, and feces)
140 collected from clinical and non-clinical animals from Farm 3. Overall, virus shedding was detected
141 more frequently in milk samples from clinical animals (24/25) with higher RNA viral loads
142 compared to non-clinical animals (1/15) (**Fig. 2A**, **Extended Data Table 2**). Clinical animals shed
143 virus at a lower frequency in nasal swabs (6/25) and urine (2/15), and no viral RNA was detected
144 in feces. (**Fig. 2A**, **Extended Data Table 2**). In non-clinical animals, viral RNA was detected in
145 6/19 nasal swabs and 4/8 urine samples (**Fig. 2A**, **Extended Data Table 2**) indicating subclinical
146 infection.

147 **Duration of H5N1 virus shedding**

148 Nasal swabs, whole blood, serum, and milk samples were collected at ~3 (n=15), 16 (n=12), and
149 31 (n=12) days post-clinical diagnosis (pcd) of HPAI to assess duration of virus shedding. On day
150 3 viral RNA was detected in nasal swabs from 2/15 animals, in whole blood of 1/15 animals, in
151 serum of 1/15 animals, and in milk of 14/15 animals (**Fig. 2B, Supplementary Data Table 2**).
152 While no virus RNA was detected in nasal swabs, whole blood, or serum samples collected on
153 days 16 and 31 pcd, milk from 10/12 and 4/12 animals tested on days 16 and 31 pcd, respectively,
154 remained positive (**Fig. 2B, Supplementary Data Table 2**). Importantly, while high infectious
155 viral loads were detected in milk on day 3 pcd ($10^{4.05}$ to $10^{8.80}$ $TCID_{50}$/mL), no infectious virus
156 was recovered from milk from days 16 and 31 pcd (**Fig. 2C**).

157 **Mammary gland tropism of H5N1 virus**

158 Histological examination of tissues from affected dairy cows revealed marked changes consisting
159 of neutrophilic and lymphoplasmacytic mastitis with prominent effacement of tubuloacinar gland

160 architecture which were filled with neutrophils admixed with cellular debris in multiple lobules in
161 the mammary gland (**Fig. 3**). The most pronounced histological changes in the cat tissues consisted
162 of mild to moderate multi-focal lymphohistiocytic meningoencephalitis with multifocal areas of
163 parenchymal and neuronal necrosis (**Extended Data Fig. 2, Extended Data Table 6**).

164 Pronounced viral RNA and antigen were detected via *in situ* hybridization (ISH) and
165 immunohistochemistry (IHC) in the mammary gland of affected cows and in the brain (cerebrum,
166 cerebellum, and brain stem) of affected cats. In mammary glands, viral RNA and antigen was
167 present in the alveolar milk-secreting epithelial cells and inter acinar spaces. In the brain of affected
168 cat, viral RNA and antigen were detected in neuronal soma glial cells, endothelial cells lining the
169 capillaries within choroid plexus, and Purkinje cells in the molecular layer of cerebellum. (**Fig 3,**
170 **Extended Data Fig. 2**). Additionally, sparce viral RNA and antigen were detected in the lung,
171 supramammary lymph nodes, spleen, heart, colon and liver from affected cows (**Extended Data**
172 **Table 3**, **Extended Data Fig. 3 and 4**). Virus infected cells were detected in peripheral areas of
173 germinal centers of lymph nodes and in cells surrounding blood vessels in the remaining tissues
174 (**Extended Data Table 3**, **Extended Data Fig. 3 and 4**). These results demonstrate a distinct
175 tropism of HPAI H5N1 virus for the mammary tissue of cattle and the central nervous system
176 tissue of cats with sporadic detection of virus infected cells in other tissues.

177 **Spillover of reassortant H5N1 virus**

178 All HPAI H5N1 sequences obtained from the farms in our study (n=91) were classified within a
179 new reassortant B3.13 genotype (**Extended Data Fig. 5**), which comprises PA, HA, NA and M
180 gene segments of an Eurasian wild bird ancestry (ea1), and NS, PB1, PB2, and NP gene segments
181 from American bird lineages (am1.1, am2.2, am4, and am8, respectively) (**Extended Data Table**
182 **4**). To identify potential parental genotypes and to define the most recent common ancestors

183 leading to the emergence of genotype B3.13, we performed Bayesian Evolutionary Analysis
184 Sampling Trees (BEAST) and TreeSort using influenza A sequences obtained between 2020-2024.
185 This analysis suggests that B3.13 genotype viruses acquired the PB2 and NP gene fragments before
186 its initial detections in avian and mammalian species in January 2024 (**Extended Data Table 4;**
187 **Extended Data Fig. 5**). The first genome segment derived from LPAI American bird lineage to
188 be incorporated in HPAI H5N1 clade 2.3.4.4b was the NS gene (am1.1); the earliest evidence of
189 its emergence derived from a reassortant genotype B3.2 virus obtained from chicken in British
190 Columbia, Canada in June of 2022 (A/chicken/BC/22-023547-001-original/2022[H5N1]);
191 **Extended Data Table 4**). Incorporation of the PB1 (am4) and PB2 (am2.2) gene segments into
192 HPAI H5N1 clade 2.3.4.4b was first detected in November 2023, in a genotype B3.9 virus
193 sequence recovered from a tundra swan (*Cygnus columbianus*) from Minnesota
194 (A/tundra_swan/Minnesota/23-037501-001-original/2023[H5N1]). The reassortant genotype
195 B3.13 virus, which incorporated the am2.2 PB2 and am8 NP gene segments, was first detected on
196 January 25, 2024 in a Canada goose (*Branta canadensis*) in Wyoming
197 (A/Canada_goose/Wyoming/24-003692-001-original/2024[H5N1]), and then in a peregrine
198 falcon (*Falco peregrinus*) in California (A/peregrine_falcon/California/24-005915-001-
199 original/2024[H5N1]) on February 14, 2024, and soon after in a skunk in New Mexico on February
200 23, 2024 (A/skunk/New_Mexico/24-006483-001-original/2024[H5N1]) (**Extended Data Table**
201 **4, Extended data Fig. 5**). The host species, in which the reassortment event culminating in the
202 incorporation of the am8 NP segment and emergence of HPAI H5N1 genotype B3.13 virus,
203 remains unknown.

204 **Phylogenomics of H5N1 B3.13 genotype**

205 Phylogenetic analysis based on concatenated whole genomes revealed that all sequences from
206 Farms 1-9, including sequences obtained from wild birds cows and other mammals, formed a large
207 monophyletic lineage (**Fig. 4A, Extended Data Fig. 6**). They were most closely related to a
208 sequence obtained from a skunk in NM on February 23, 2024 (A/skunk/New_Mexico/24-006483-
209 001-original/2024). The sequences obtained from the affected dairy farms characterized in the
210 present study formed two large phylogenetic branches, with the largest one including three
211 subclusters. Notably, these phylogenetic groups of closely related sequences were not always
212 formed by sequences derived from the same farm (**Fig. 4B**). Phylogenetic branches formed by
213 sequences obtained from cattle from Farms 1 and 3, Farms 1 and 8, and Farms 7 and 9 suggested
214 a close genetic relationship between the viruses in these farms (**Fig. 4B**), and potential transfer of
215 the virus between farms. Similarly, sequences obtained from cattle from Sites 1 and 2 of Farm 2
216 (a multi-site dairy operation), formed a monophyletic cluster, indicating co-circulation of the virus
217 in these two sites (**Fig. 4B**).

218 Next, the mutation profile of HPAI H5N1 clade 2.3.4.4b was investigated. Initially, we
219 evaluated the occurrence of mutations with known functional relevance to IAV (e.g. host
220 adaptation, virulence, host specificity shift, etc.) in comparison to the original H5N1
221 A/GsGd/1/1996 virus (**Supplementary Data Table 3**). Further we performed a detailed
222 comparative genome analysis and mutational profiling using sequences obtained in the U.S.
223 throughout the 2021-2024 HPAI outbreak (**Extended Data Table 5**). The sequence
224 A/chicken/NL/FAV-0033/2021 2.3.4.4b was used as a reference to identify mutations in different
225 genome segments across affected species. Representative sequences from multiple genotypes (A1,
226 A2, B1.3, B3.2, Minor01, B3.6, B3.9 and B3.13) were selected, including sequences from avian
227 (chicken and great tailed grackle) and mammalian (skunk, red fox, harbor seals, human, goat, cat,

228 and cattle) hosts. A total of 132 amino acid substitutions were observed across the 8 genome
229 segments, most of which are low frequency mutations observed in a small proportion of cattle
230 derived viral sequences (**Extended Data Table 5, Supplementary Data Table 6**). Fifteen
231 mutations emerged in viruses of genotypes (e.g. A2, and B3.6) circulating in late 2023 and were
232 maintained in genotype B3.13 viruses in 2024 including mutations in PB2 (V109I, V139I, V495I,
233 and V649I), PB1 (E75D, M171V, R430K, and A587P), PA (K113R), HA (T211I), NA (V67I,
234 L269M, V321I, and S339P), NP (S482N), and NS1 (C116S) genes. Seven additional mutations
235 were detected exclusively in genotype B3.13 viruses including five substitutions in PB2 (T58A,
236 E362G, D441N, M631L, and T676A) one in PA (L219I) and one in NS1 (S7L). When compared
237 to the first reported B3.13 sequences (A/Canada_goose/Wyoming/24-003692-001-
238 original/2024[H5N1]), A/peregrine_falcon/California/24-005915-001-original/2024[H5N1] and
239 A/skunk/New_Mexico/24-006483-001-original/2024[H5N1]), the cow HPAI H5N1 virus
240 sequences presented five amino acid substitutions, including: three in PB2 (E362G, D441N and
241 M631L), one in PA (L219I) and one in NS (S7L) (**Extended Data Table 5**), suggesting that these
242 could have emerged following spillover in cattle.

243 **H5N1 virus dispersal between farms**

244 The HPAI H5N1 genotype B3.13 sequences obtained from farms presenting an epidemiological
245 link (Farm 2: separate production sites [site 1 and 2]; and Farms 1 and 3: animals were transported
246 from Farm 1 to 3) (**Extended Data Table 1**) or presenting closely related viral sequences (7 and
247 9) (**Fig. 4B**) were subjected to phylogeographic dispersal reconstructions (**Fig. 5A**). Haplotype
248 network analysis of concatenated whole genome sequences provided support for focusing the
249 dispersal and phylogeographical inferences on Farms 1 and 3, Farm 2, and Farms 7 and 9 (**Fig.
250 5B**). The phylogenetic relationship and dispersal pathways were inferred based on concatenated

251 whole genome sequences, the farm location and date of sample collection to reconstruct
252 hypothetical dispersal trajectories of HPAI virus between the farms. The viral sequences recovered
253 from Farm 2, which were collected from two separated production sites (1 and 2, approximately
254 50 Km apart), formed two phylogenetic clusters, each comprising sequences from both sites,
255 confirming the spread of the virus between these premises. Phylogeographical dispersal analysis
256 of the HPAI H5N1 sequences recovered from Farm 2, suggest site 1 as the likely source of the
257 virus (**Fig. 5C**).

258 Viral sequences obtained from Farms 7, and 9 (six sequences from Farm 7 and 11
259 sequences from Farm 9), which are ~280 Km apart from each other, formed a monophyletic cluster
260 suggesting a link and potential bidirectional virus dispersal between these two farms (**Fig. 5D**).
261 However, another hypothesis that cannot be formally excluded as it could not be resolved by our
262 analysis is unidirectional dispersal of multiple viral lineages from Farm 7 to 9 or vice versa. Given
263 the close genetic relationship between the viruses in these farms, we conducted a broader
264 phylogenetic analysis including other HPAI H5N1 B3.13 sequences available in GISIAD. This
265 analysis revealed two additional H5N1 sequences recovered from blackbirds (unknown species)
266 clustering with viral sequences from Farm 7 and 9 (**Extended Data Fig. 7)**. Importantly, the
267 blackbirds were collected at 8-12 Km away from Farm 7. Together these results suggest both
268 long- and close-range lateral spread and transmission of HPAIV between farms.

269 Sequences obtained from Farms 1 (TX) and 3 (OH) branched interspersedly in two
270 subclusters. Viral sequence recovered from animals from Farm 1 were basal to all sequences from
271 Farm 3. Phylogeographic dispersal analysis revealed that HPAIV most likely spread from Farm 1
272 (TX) to Farm 3 (OH) (**Fig. 5E**). This is consistent with the epidemiological information revealing
273 the transportation of 42 apparently healthy dairy cattle from Farm 1 to Farm 3 on March 8, 2024,

274 five days before the first clinical signs were observed in animals in Farm 1 and 12 days before the
275 first clinical animal was identified in Farm 3 (**Extended Data Table 1**). These results indicate
276 transmission of HPAI H5N1 between subclinically infected cows.

277 **Interspecies transmission of H5N1 virus**

278 Given that five of the nine farms included in our study (Farms 1, 3, 4, 5, and 8) reported mortality
279 events in wild (great-tailed grackles) and peri-domestic birds (pigeons), and in wild (raccoon) and
280 domestic mammals (cats), we investigated potential HPAI infection in these species. Whole
281 genome sequencing of the samples from the grackles and a cat from Farm 1 and a raccoon from
282 Farm 8 confirmed infection of these species with a HPAI H5N1 genotype B3.13 virus closely
283 related to the viruses found in dairy cattle in these farms. The basal sequences for the viruses
284 obtained from a cat in Farm 1 and the raccoon in Farm 8 were derived from dairy cattle, indicating
285 cattle-to-cat and cattle-to-raccoon transmission (**Extended Data Fig. 8**). This is supported by
286 epidemiological information revealing that feeding raw milk to farm cats was a common practice
287 in these farms.

288 **Discussion**

289 Here we describe the spillover of a new reassortant HPAI H5N1 clade 2.3.4.4b genotype
290 B3.13 virus into dairy cattle and provide evidence of efficient transmission among cattle and
291 between cattle and other species, highlighting the virus' ability to cross species barriers. The farms
292 that first reported and confirmed HPAI H5N1 genotype B3.13 infection in cattle in TX, NM, and
293 KS are on the Central North American migratory bird flyway. Importantly, the first reported
294 genome sequence of genotype B3.13 virus was obtained from a sample collected from a Canada
295 goose in Wyoming (January 25, 2024), within the same flyway. This was followed by a detection
296 in a peregrine falcon in California (CA) (February 14, 2024) on the Pacific flyway, and then in a

297 skunk in NM (February 23, 2024), again on the Central flyway. The lack of complete
298 epidemiological information regarding the H5N1 genotype B3.13 sequence collected from the
299 skunk in NM precludes definitive conclusions on the link of this animal with affected dairy cattle
300 farms in the region. However, this findings demonstrate the presence of the virus in wildlife in
301 NM around the same time (January-February, 2024) that the first cases of sick cows presenting
302 mild respiratory signs, drop in feed intake, and milk production (which were later confirmed to be
303 caused by HPAI H5N1 genotype B3.13) were reported[35]. Additional historic and prospective
304 sequence data are needed for more detailed molecular epidemiological inferences.

305 Our results demonstrate a high tropism of HPAI H5N1 for the mammary gland tissue
306 resulting in a viral-induced mastitis, which was confirmed by histological changes and direct viral
307 detection *in situ* demonstrating viral replication and defining the virus tropism for milk-secreting
308 mammary epithelial cells lining the alveoli in the mammary gland. The tropism of HPAI H5N1
309 for milk-secreting epithelial cells is consistent with high expression of sialic acid receptors with
310 an α2,3 (avian-like receptor) and α2,6 (human-like receptor) galactose linkage in these cells[36].
311 Although the tissue sample size included in our study was small, isolation of the virus in lung and
312 suprammamary lymph nodes (which were also positive for viral RNA and antigen) suggests that
313 other organs may also play a role in the virus infection dynamics and pathogenesis in dairy cattle.
314 The initial site of virus replication remains unknown; however, it is possible that the virus infects
315 through respiratory and/or oral routes replicating at low levels in the upper respiratory tract (e.g.
316 nasal turbinate, trachea, and/or pharynx), from where it could disseminate to other organs via a
317 short and low-level viremia. The collected evidence suggests that the mammary gland is the main
318 site of virus replication, resulting in substantial virus shedding in milk. Another possible
319 transmission route includes direct infection of the mammary gland through the teat orifice and

320 cisternae, which could occur through contaminated floors and bedding were animals lay in the
321 farm or mechanically via the milking equipment during milking. This entry route could also lead
322 to viremia and subsequent virus dissemination/replication in other distant tissue sites. In the 1950's
323 several studies showed that direct inoculation of virus into the udder of dairy cows and goats with
324 the human PR8 strain of type A influenza led to infection and viral shedding[37–41]. These results
325 suggests, considering the current outbreak, that mammary epithelial cells, which express α2,3 and
326 α2,6 sialic acid[36], may be generally susceptible to influenza A viruses. There are a few studies
327 suggesting an association between influenza A and clinical disease[42–47], but there is no evidence
328 of sustained transmission. The only published study of a goose/Guangdong lineage virus being
329 inoculated intranasally into calves showed limited viral replication with no clinical disease and no
330 evidence of transmissioin[48]. Experimental infection studies using different inoculation routes (i.e.
331 intranasal *vs* intramammary) with HPAI H5N1 genotype B3.13 virus and, perhaps, other
332 contemporary viruses of the 2.3.4.4b lineage in dairy cattle with sequential and comprehensive
333 sampling are critical to answer these important questions about the port of entry, infection
334 dynamics and pathogenesis in this new host species.

335 Spillover of HPAI H5N1 clade 2.3.4.4b into mammalian species has been reported
336 throughout the current global outbreak[20,49]; however there is no evidence of sustained virus
337 transmission in mammals. Our epidemiological investigation combined with genome sequence-
338 and geographical dispersal analysis provides evidence of efficient intra- and inter-species
339 transmission of HPAI H5N1 genotype B3.13. Soon after apparently healthy lactating cattle were
340 moved from Farm 1 to Farm 3, resident animals in Farm 3 developed clinical signs compatible
341 with HPAI H5N1 providing evidence to suggest that non-clinical animals can spread the virus.
342 Analysis of the genetic relationship between the viruses detected in Farms 1 and 3, combined with

343 phylogeographical modeling indicate that the viruses infecting cattle in these farms are closely
344 related, supporting the direct epidemiological link and indicating long-range viral dispersal and
345 efficient cattle-to-cattle transmission. The results from the phylogenomic and phylogeographical
346 analyses in both sites of Farm 2 and on Farms 7 and 9 also indicate regional long-range farm-to-
347 farm spread of the virus. In these cases, fomites such as shared farm equipment, vehicles, or
348 personnel may have played a role in virus spread. The dispersal of virus between Farms 7 and 9
349 could have been vectored by wild birds; as suggested by the fact that blackbirds found dead near
350 Farm 7 were infected with a virus closely related to the virus circulating in cattle in these farms.
351 Alternatively, the birds at this premise could have been infected with virus shed by cattle. All
352 affected farms from this study are large farms with cattle maintained in open air pens which
353 facilitates access of wild birds or mammals to feed and water, which could mediate indirect contact
354 between cattle and wild birds. Our phylogenomic analysis in sequences recovered from affected
355 cats (Farms 1, 2, 4, and 5) and a raccoon (Farm 8) combined with epidemiological information
356 revealing the practice of feeding raw milk to cats in these farms support cattle-to-cat and cattle-to-
357 raccoon transmission. These observations highlight complex pathways underlying the introduction
358 and spread of HPAI H5N1 in dairy farms (**Fig. 6**), underscoring the need for efficient biosecurity
359 practices and enhanced surveillance efforts in affected and non-affected farms.

360 The spillover of HPAI H5N1 into dairy cattle and evidence for efficient and sustained
361 mammal-to-mammal transmission are unprecedented. This efficient transmission is concerning as
362 it can lead to the adaptation of the virus, potentially enhancing its infectivity and transmissibility
363 in other species, including humans. Although none of the nine affected farms included in the
364 present study reported cases of human HPAI H5N1 infection, there have been three confirmed
365 human cases resulting in mild conjunctivitis and respiratory infection in other farms in Texas and

Michigan[50–52]. These cases highlight the zoonotic potential of the virus underscoring the need for robust measures to prevent and control the infection and further spread of HPAI H5N1 in dairy cattle. This would reduce the risk of the virus adapting in this new mammalian host species, thereby decreasing the pandemic risk to humans.

References

1. Kandeil, A. *et al.* Rapid evolution of A(H5N1) influenza viruses after intercontinental spread to North America. *Nat. Commun.* **14**, 1–13 (2023).
2. Youk, S. *et al.* H5N1 highly pathogenic avian influenza clade 2.3.4.4b in wild and domestic birds: Introductions into the United States and reassortments, December 2021–April 2022. *Virology* **587**, 109860 (2023).
3. USDA-APHIS, in Detections of Highly Pathogenic Avian Influenza in Wild Birds. https://www.aphis.usda.gov/livestock-poultry-disease/avian/avian-influenza/hpai-detections/wild- birds (2024).
4. USDA-APHIS, in Confirmations of Highly Pathogenic Avian Influenza in Commercial and Backyard Flocks. https://www.aphis.usda.gov/livestock-poultry-disease/avian/avian-influenza/hpai-detections/commercial-backyard-flocks (2024).
5. Puryear, W. *et al.* Highly Pathogenic Avian Influenza A(H5N1) Virus Outbreak in New England Seals, United States. *Emerg. Infect. Dis.* **29**, 786–791 (2023).
6. Cronk, B. D. *et al.* Infection and tissue distribution of highly pathogenic avian influenza A type H5N1 (clade 2.3.4.4b) in red fox kits (Vulpes vulpes). *Emerg. Microbes Infect.* **12**, (2023).
7. Rijks, J. M. *et al.* Highly Pathogenic Avian Influenza A(H5N1) Virus in Wild Red Foxes, the Netherlands, 2021. *Emerg. Infect. Dis.* **27**, 2960–2962 (2021).
8. Bordes, L. *et al.* Highly Pathogenic Avian Influenza H5N1 Virus Infections in Wild Red Foxes (Vulpes vulpes) Show Neurotropism and Adaptive Virus Mutations. *Microbiol. Spectr.* **11**, e0286722 (2023).
9. Plaza, P. I., Gamarra-Toledo, V., Rodríguez Euguí, J., Rosciano, N. & Lambertucci, S. A. Pacific and Atlantic sea lion mortality caused by highly pathogenic Avian Influenza A(H5N1) in South America. *Travel Med. Infect. Dis.* **59**, 102712 (2024).
10. Alkie, T. N. *et al.* Characterization of neurotropic HPAI H5N1 viruses with novel genome constellations and mammalian adaptive mutations in free-living mesocarnivores in Canada. *Emerg. Microbes Infect.* **12**, 2186608 (2023).
11. Jakobek, B. T. *et al.* Influenza A(H5N1) Virus Infections in 2 Free-Ranging Black Bears (Ursus americanus), Quebec, Canada. *Emerg. Infect. Dis.* **29**, 2145–2149 (2023).
12. Sillman, S. J., Drozd, M., Loy, D. & Harris, S. P. Naturally occurring highly pathogenic avian influenza virus H5N1 clade 2.3.4.4b infection in three domestic cats in North America during 2023. *J. Comp. Pathol.* **205**, 17–23 (2023).

13. Ellis, T. M. *et al.* Investigation of outbreaks of highly pathogenic H5N1 avian influenza in waterfowl and wild birds in Hong Kong in late 2002. *Avian Pathol.* **33**, 492–505 (2004).
14. Xu, X., Subbarao, Cox, N. J. & Guo, Y. Genetic characterization of the pathogenic influenza A/Goose/Guangdong/1/96 (H5N1) virus: similarity of its hemagglutinin gene to those of H5N1 viruses from the 1997 outbreaks in Hong Kong. *Virology* **261**, 15–19 (1999).
15. Ali, M. *et al.* Genetic Characterization of Highly Pathogenic Avian Influenza A(H5N8) Virus in Pakistani Live Bird Markets Reveals Rapid Diversification of Clade 2.3.4.4b Viruses. *Viruses* **13**, (2021).
16. de Vries, E. *et al.* Rapid Emergence of Highly Pathogenic Avian Influenza Subtypes from a Subtype H5N1 Hemagglutinin Variant. *Emerg. Infect. Dis.* **21**, 842–846 (2015).
17. Lee, K. *et al.* Characterization of highly pathogenic avian influenza A (H5N1) viruses isolated from cats in South Korea, 2023. *Emerg. Microbes Infect.* **13**, 1–4 (2024).
18. Adlhoch, C. *et al.* Avian influenza overview March - April 2023. *EFSA journal. Eur. Food Saf. Auth.* **21**, e08039 (2023).
19. Harvey, J. A., Mullinax, J. M., Runge, M. C. & Prosser, D. J. The changing dynamics of highly pathogenic avian influenza H5N1: Next steps for management & science in North America. *Biol. Conserv.* **282**, 110041 (2023).
20. Elsmo, E. *et al.* Highly Pathogenic Avian Influenza A(H5N1) Virus Clade 2.3.4.4b Infections in Wild Terrestrial Mammals, United States, 2022. *Emerg. Infect. Dis. J.* **29**, 2451 (2023).
21. Tammiranta, N. *et al.* Highly pathogenic avian influenza A (H5N1) virus infections in wild carnivores connected to mass mortalities of pheasants in Finland. *Infect. Genet. Evol. J. Mol. Epidemiol. Evol. Genet. Infect. Dis.* **111**, 105423 (2023).
22. Ulloa, M. *et al.* Mass mortality event in South American sea lions (Otaria flavescens) correlated to highly pathogenic avian influenza (HPAI) H5N1 outbreak in Chile. *Vet. Q.* **43**, 1–10 (2023).
23. Agüero, M. *et al.* Highly pathogenic avian influenza A(H5N1) virus infection in farmed minks, Spain, October 2022. *Eurosurveillance* **28**, (2023).
24. World Health Organization. Cumulative number of confirmed human cases for avian influenza A(H5N1) reported to WHO, 2003-2024, 28 March 2024. https://www.who.int/publications/m/item/cumulative-number-of-confirmed-human-cases-for-avian-influenza-a(h5n1)-reported-to-who--2003-2024-28-march-2024 (2024).
25. de Jong, M. D. & Hien, T. T. Avian influenza A (H5N1). *J. Clin. Virol.* **35**, 2–13 (2006).
26. Sutton, T. C. The Pandemic Threat of Emerging H5 and H7 Avian Influenza Viruses. *Viruses* **10**, (2018).
27. Caliendo, V. *et al.* Transatlantic spread of highly pathogenic avian influenza H5N1 by wild birds from Europe to North America in 2021. *Sci. Rep.* **12**, 11729 (2022).
28. Bevins, S. *et al.* Intercontinental Movement of Highly Pathogenic Avian Influenza A(H5N1) Clade 2.3.4.4 Virus to the United States, 2021. *Emerg. Infect. Dis. J.* **28**, 1006 (2022).
29. USDA-APHIS. Detections of Highly Pathogenic Avian Influenza. https://www.aphis.usda.gov/livestock-poultry-disease/avian/avian-influenza/hpai-detections (2024).
30. Plaza, P. I., Gamarra-Toledo, V., Euguí, J. R. & Lambertucci, S. A. Recent Changes in Patterns of Mammal Infection with Highly Pathogenic Avian Influenza A(H5N1) Virus

Worldwide. *Emerg. Infect. Dis.* **30**, 444–452 (2024).
31. Lisa Schnirring. Avian flu detected again in Antarctic penguins. https://www.cidrap.umn.edu/avian-influenza-bird-flu/avian-flu-detected-again-antarctic-penguins (2024).
32. U.S. Case of Human Avian Influenza A(H5) Virus Reported. https://www.cdc.gov/media/releases/2022/s0428-avian-flu.html (2022).
33. Shu, Y. & McCauley, J. GISAID: Global initiative on sharing all influenza data - from vision to reality. *Euro surveillance : bulletin Europeen sur les maladies transmissibles = European communicable disease bulletin* vol. 22 (2017).
34. Lisa Schnirring. Avian flu detected for first time in US livestock. https://www.cidrap.umn.edu/avian-influenza-bird-flu/avian-flu-detected-first-time-us-livestock (2024).
35. Federal and State Veterinary, Public Health Agencies Share Update on HPAI Detection in Kansas, Texas Dairy Herds. https://www.aphis.usda.gov/news/agency-announcements/federal-state-veterinary-public-health-agencies-share-update-hpai (2024).
36. Kristensen, C., Larsen, L. E., Trebbien, R. & Jensen, H. E. The avian influenza A virus receptor SA-α2,3-Gal is expressed in the porcine nasal mucosa sustaining the pig as a mixing vessel for new influenza viruses. *Virus Res.* **340**, 199304 (2024).
37. Mitchell, C. A., Nordland, O. & Walker, R. V. L. Myxoviruses and Their Propagation in the Mammary Gland of Ruminants. *Can. J. Comp. Med.* **XXII**, 154–156 (1958).
38. Mitchell, C. A., Walker, R. V. L. & Bannister, G. L. Further experiments relating to the propagation of virus in the bovine mammary gland. *Can. J. Comp. Med.* **XVII**, 218–222 (1953).
39. Mitchell, C. A., Walker, R. V. L. & Bannister, G. L. Persistence of neutralizing antibody in milk and blood of cows and goats following the instillation of virus into the mammary gland. *Can. J. Comp. Med.* **XVIII**, 426–430 (1954).
40. Mitchell, C. A., Walker, R. V., & Bannister, G. L. Preliminary Experiments Relating to the Propagation of Viruses in the Bovine Mammary Gland. *Can. J. Comp. Med. Vet. Sci.* **17**, 97–104 (1953).
41. MITCHELL CA, WALKER RV, B. G. Studies relating to the formation of neutralizing antibody following the propagation of influenza and Newcastle disease virus in the bovine mammary gland. *Can J Microbiol.* **2**, 322–8 (1956).
42. Sreenivasan, C. C., Thomas, M., Kaushik, R. S., Wang, D. & Li, F. Influenza A in Bovine Species: A Narrative Literature Review. *Viruses* **11**, (2019).
43. Campbell, C. H., Easterday, B. C. & Webster, R. G. Strains of Hong Kong influenza virus in calves. *J. Infect. Dis.* **135**, 678–680 (1977).
44. Hu, X. *et al.* Highly Pathogenic Avian Influenza A (H5N1) clade 2.3.4.4b Virus detected in dairy cattle. *bioRxiv* (2024).
45. Gunning, R. F., Brown, I. H. & Crawshaw, T. R. Evidence of influenza a virus infection in dairy cows with sporadic milk drop syndrome. *Vet. Rec.* **145**, (1999).
46. Brown, I. H., Crawshaw, T. R., Harris, P. A. & Alexander, D. J. Detection of antibodies to influenza A virus in cattle in association with respiratory disease and reduced milk yield. *Vet. Rec.* **143**, (1998).
47. Graham, D. A., Calvert, V. & McLaren, I. E. Retrospective analysis of serum and nasal mucus from cattle in Northern Ireland for evidence of infection with influenza A virus. *Vet. Rec.* **150**, (2002).

48. Kalthoff, D., Hoffmann, B., Harder, T., Durban, M. & Beer, M. Experimental infection of cattle with highly pathogenic avian influenza virus (H5N1). *Emerg. Infect. Dis.* **14**, (2008).
49. Arruda, B. *et al.* Divergent Pathogenesis and Transmission of Highly Pathogenic Avian Influenza A(H5N1) in Swine. *Emerg. Infect. Dis.* **30**, (2024).
50. Uyeki, T. M. *et al.* Highly Pathogenic Avian Influenza A(H5N1) Virus Infection in a Dairy Farm Worker. *The New England journal of medicine* (2024) doi:10.1056/NEJMc2405371.

Figure Legends

Fig. 1 | Detection and isolation of HPAI H5N1 from dairy cattle. a, Viral RNA loads in nasal swab (n=27), whole blood (n=25), serum (n=15), urine (n=4), feces (n=10), and milk (n=167) samples collected from cattle from Farms 1-9 quantified by rRT-PCR targeting the influenza A virus matrix gene. **b**, Viral RNA loads in tissues of dairy cattle quantified by rRT-PCR targeting the influenza A virus matrix gene. **c**, Serum antibody responses in affected cattle (n=19) quantified by hemagglutination inhibition (HI) assay. **d**, Cytopathic effect of HPAI H5N1 virus from milk in bovine uterine epithelial cells Cal-1. The photomicrograph shown is representative of two independent clinical samples. Scale bar 50 µm. **e**, Detection of infectious HPAI virus in Cal-1 cells by immunofluorescence assay using a nucleoprotein specific monoclonal antibody (red) counterstained stained with 4′,6-diamidino-2-phenylindole (Blue). The photomicrograph shown is representative of two independent clinical samples. Scale bar 50 µm.Added Infectious HPAI virus in milk (n=69) **f** and tissues **g** detected by virus titration. Virus titers were determined using endpoint dilutions and expressed as $TCID_{50}.mL^{-1}$. The limit of detection (LOD) for infectious virus titration was $10^{1.05}$ $TCID_{50}.mL^{-1}$. Data are presented as mean values ± SEM. All graphs and statistical analysis were generated using GraphPad Prism, version 10

527 **Fig. 2 | Virus shedding patterns. a**, Viral shedding and RNA load in milk (n=41), nasal swabs
528 (n=45), urine (n=23) and feces (n=25) collected from clinical and non-clinical animals from an
529 HPAI affected farm. **b**, Viral RNA loads in milk samples collected from cattle from Farm 3 on
530 days 3 (n=15), 16 (n=12) and 31 (n=9) post-clinical diagnosis quantified by rRT-PCR targeting
531 the influenza A virus matrix gene. **c**, Infectious HPAI virus in milk (n=13 per time point)
532 detected by virus titration. Virus titers were determined using endpoint dilutions and expressed
533 as $TCID_{50}.mL^{-1}$. The limit of detection (LOD) for infectious virus titration was $10^{1.05}$
534 $TCID_{50}.mL^{-1}$. Data are presented as mean values ± SEM. All graphs and statistical analysis were
535 generated using GraphPad Prism, version 10.
536 **Fig. 3 | Detection of HPAI H5N1 in dairy cattle mammary gland tissue.** Hematoxylin and
537 eosin (H&E) staining (left panels) showing intraluminal epithelial sloughing and cellular debris
538 in mammary alveoli (Z1 and Z2). Normal mammary alveoli filled with milk and fat globules
539 (Z3). In situ hybridization (ISH) (middle panels) targeting Influenza A virus (Matrix gene)
540 showing extensive viral RNA in milk-secreting epithelial cells in the alveoli and in intraluminal
541 cellular debris (Z1 and Z2). Normal mammary alveoli showing no viral staining (Z3).
542 Immunohistochemistry (IHC) (right panels) targeting Influenza A virus M gene showing
543 intracytoplasmic immunolabeling of viral antigen in milk secreting alveolar epithelial cells (Z1
544 and Z2). Normal mammary alveoli showing no viral staining (Z3).
545
546 **Fig. 4 | Phylogenetic analysis of HPAI H5N1. a**, Phylogeny of sequences derived from cattle,
547 cats, raccoon, and grackle sampled in the farms described in this study, and other sequences in
548 closer ancestral branches, obtained from GISAID database. Nodes are colored by host species. **b**,
549 Detailed view of the clade containing 91 sequences derived from animals sampled in the farms

550 described in this study. Nodes are colored by farm. All phylogenomic analyses were conducted
551 with concatenated whole genome sequences.
552
553 **Fig. 5 | Interstate and local dispersal of HPAI H5N1 genotype B3.13 between farms. a**,
554 HPAI H5M1 dispersal in North America. Samples described in this study are colored by farm,
555 while locations in grey represent samples from closer ancestral branches obtained from GISAID
556 database. **b**, Haplotype network analysis of HPAI H5N1 viral sequences obtained from the farms
557 described in this study. Different colors indicate different farms. The size of each vertex is
558 relative to the number of samples and the dashes on branches show the number of mutations
559 between nodes. Phylogenetic reconstruction and analysis of dispersal between Sites 1 and 2 of
560 farm 2 (**c**), Farms 7 and 9 (**d**), and Farms 1 and 3 (**e**). Directions of dispersal lines are
561 counterclockwise. All phylogenomic and dispersal analyses were conducted with concatenated
562 whole genome sequences.
563
564 **Fig. 6 | Model of spillover and spread of HPAI H5N1 genotype B3.13 into dairy cattle.** A
565 reassortment event in an unknown host species led to the emergence of H5N1 genotype B3.13
566 which circulated in wild birds and mammals before infecting dairy cattle. Following spillover of
567 H5N1 into dairy cattle, the virus was able to establish infection and efficiently transmit from
568 cow-to-cow (intraspecies transmission) and from cow to other species, including wild (great
569 tailed grackles) and peridomestic birds (pigeons) and mammals (cats and raccoons) (interspecies
570 transmission). Spread of the virus between farms occurred by the movement of cattle between
571 farms, and likely by movement wild birds and fomites including personnel, shared farm

572 equipment and trucks (feed, milk and/or animal trucks). Figure was created using
573 BioRender.com.
574
575 **Methods**
576 **Inclusion and ethics statement**
577 All authors of this study were committed to high standards of inclusion and ethics in research.
578 Clinical samples used in the present study were collected as part of routine diagnostic procedures
579 and the data used for research. The findings of this study are reported transparently, with a
580 commitment to accuracy and integrity. All data and results are presented without manipulation,
581 and any limitations of the study are clearly acknowledged.
582 **Sample collection**
583 Clinical samples used in the present study were collected by field veterinarians from nine clinically
584 affected farms in TX (Farm 1, 2, 4, 5, 6 and 7), NM (Farm 8), KS (Farm 9) or OH (Farm 3). A
585 total of 332 samples collected from dairy cattle (n=323), domestic cats (n=4), great-tailed grackles
586 (n=3), pigeon (n=1) and a racoon (n=1) in the affected farms. All samples including milk (n=211),
587 nasal swabs (n=46), whole blood (n=25), serum (n=15), feces (n=10), urine (n=4), and tissues
588 (mammary gland [n=4], lung [n=1], lymph nodes [n=3], small [n=3] and large intestine [n=1])
589 from dairy cattle were submitted to the Cornell Animal Health Diagnostic Center (AHDC), Texas
590 A&M Veterinary Medical Diagnostic Laboratory (TVMDL) or the Ohio Animal Disease
591 Diagnostic Laboratory (OADDL) for diagnostic investigations. One domestic cat, two grackles
592 and one pigeon (Farm 1) were submitted to the AHDC while three cats (Farms 4 and 8) and a
593 racoon (Farm 8) and four cows were submitted to TVMDL for necropsy and testing
594 (**Supplementary Data Table 1**).

595 Sequential samples (milk, nasal swabs and blood) collected from animals (n=15) from
596 Farm 3 were used to investigate duration of virus shedding (**Supplementary Data Table 2**).
597 Additionally, paired samples (milk, nasal sabs, urine and feces) collected from animals presenting
598 respiratory distress, drop in milk production and altered milk characteristics (clinical, n=25) and
599 from apparently healthy animals (non-clinical, n=20) from Farm 3 were used to compare virus
600 shedding by clinical and non-clinical animals (**Extended Data Table 2**).

601 **Clinical history and epidemiological information**

602 Clinical history from all nine farms were obtained from the sample submission forms sent with the
603 samples to the AHDC, TVMDL and OADDL. Additional relevant information from each farm
604 were obtained from attending veterinarians through investigations conducted by laboratory
605 diagnosticians.

606 **Real-time reverse transcriptase PCR (rRT-PCR)**

607 Viral nucleic acid was extracted from milk, nasal swabs, whole blood, serum, feces, urine and
608 tissue homogenates. Two hundred µl of milk, nasal swabs, whole blood, serum, and urine were
609 used for extraction. Two hundred µl of raw milk samples were used directly or diluted at the ratio
610 of 1 part of milk to 3 parts of phosphate-buffered saline (PBS) with 200 µl of the dilution used for
611 nucleic acid extraction. Tissues and feces were homogenized in PBS-BSA (1%) (10% w/v),
612 cleared by centrifugation and 200 µl of the supernatant were used for extraction. All RNA
613 extractions were performed using the MagMAX Pathogen RNA/DNA Kit (Thermo Fisher,
614 Waltham, MA, USA) and the automated King Fisher Flex nucleic acid extractor (Thermo Fisher,
615 Waltham, MA, USA) following the manufacturer's recommendations. The presence of IAV RNA
616 was assessed using the VetMax-Gold AIV Detection Kit (Thermo Fisher, Waltham, MA, USA)
617 and the National Animal Laboratory Network (NAHLN) primers and probe targeting the

618 conserved M gene or the H5 hemagglutinin gene[53]. Amplification and detection were performed
619 using the Applied Biosystems 7500 Fast PCR Detection System (Thermo Fisher, Waltham, MA,
620 USA), under following conditions: 10 min at 45ºC for reverse transcription, 10 min at 95 °C for
621 polymerase activation and 45 cycles of 15 s at 94 °C for denaturation and 30 s at 60 °C for
622 annealing and extension. Relative viral loads were calculated and are expressed as 45 rRT-PCR
623 cycles minus the actual CT value (45-Ct). Positive and negative amplification controls as well as
624 internal inhibition controls were run side by side with test samples. Part of samples was also tested
625 using 200 µl of undiluted milk and serum, and 100 µl of whole blood, targeting the M gene. These
626 samples were extracted using the IndiMag Pathogen kit (INDICAL Bioscience) on the KingFisher
627 Flex (Thermo Fisher, Waltham, MA, USA), and the rRT-PCR was performed using the Path-ID™
628 Multiplex One-Step RT-PCR Kit (Thermo Fisher, Waltham, MA, USA) under following
629 conditions: 10 min at 48ºC, 10 min at 95 °C, 40 cycles of 15 s at 95 °C for denaturation and 60 s
630 at 60 °C.

631 **Hemagglutination inhibition (HI)**

632 Paired serum samples collected during acute and convalescent phase of infection from animals
633 (n=20) from Farm 2, were used to determine seroconversion to HPAI H5N1 virus using the HI
634 test. Serum HI activity was determined using BPL inactivated A/Tk/IN/3707/22 antigen (clade
635 2.3.4.4b), as described previously. HI titers are expressed as log2 values, with 1 log2 being the
636 minimum titer considered positive.

637 **Virus isolation**

638 Virus isolation was performed in pooled milk samples from Farms 1 and 2. Approximately 5 ml
639 of milk from individual animals were pooled and a total of 50 ml of pooled milk were centrifuged
640 at 1,700 x g for 10 min at 4ºC. The supernatant was discarded, and the pellet was resuspended in

641 5 ml of sterile PBS-BSA (1%) followed by centrifugation at 1,700 x g for 10 min at 4ºC. The wash
642 step was repeated one more time and the final pellet was resuspended in 1 ml PBS-BSA (1%).
643 Virus isolation was conducted in bovine uterine epithelial cells (CAL-1, developed in house at the
644 Virology Laboratory at AHDC) cultured in minimal essential medium (MEM, Corning Inc.,
645 Corning, NY) supplemented with 10% fetal bovine serum (FBS) and penicillin-streptomycin
646 (Thermo Fisher Scientific, Waltham, MA; 10 $U.mL^{-1}$and 100 $\mu g.mL^{-1}$, respectively). Cells were
647 cultured in T25 flasks and inoculated with 1 mL of the milk pellet resuspension from infected cows
648 and incubated at 37 °C for 1 hour (adsorption). The inoculum was then removed, and cells were
649 washed once with phosphate buffered saline and replenished with 1 mL complete growth media
650 (MEM 10% FBS). Cells were monitored daily for the development of cytopathic effects (CPE)
651 including cell swelling, rounding and detachment. When the CPE reached 70-80%, infected cells
652 were harvested, and cell suspensions were collected after three freeze-thaw cycles. The identity of
653 the isolated virus was confirmed by rRT-PCR, an immunofluorescence assay (IFA) using anti-
654 nucleoprotein mouse monoclonal antibody (HB65, ATCC, H16-L10-4R5) and whole genome
655 sequencing. Cell nuclei were stained with 4′,6-diamidino-2-phenylindole (DAPI) (ThermoFisher
656 Scientific, 62248).

657 **Virus titrations**

658 The infectious viral loads in milk and tissues of infected animals were quantified by viral titrations.
659 For this, serial 10-fold dilutions of rRT-PCR positive milk samples and tissue homogenates were
660 prepared in MEM and inoculated into CAL-1 cells in 96-well plates. Each dilution was inoculated
661 in quadruplicate wells. At 48h post-inoculation, culture supernatant was aspirated, and cells were
662 fixed with 3.7% formaldehyde solution for 30 min at RT and subjected to IFA using the anti-NP

663 (HB65) mouse monoclonal antibody. Virus titers were determined using end-point dilutions and
664 the Spearman and Karber's method and expressed as $TCID_{50}.mL^{-1}$.

665 **Microscopic changes, in situ hybridization (ISH) and immunohistochemistry (IHC)**

666 A total of 25 tissue samples from four dairy cattle and 12 tissues from one domestic cat were
667 collected and fixed in formalin. This formalin fixed paraffin embedded (FFPE) tissues were
668 sectioned at 3 µm thickness, stained with hematoxylin and eosin (H&E), and examined for
669 histological changes. To determine the virus tropism and tissue distribution in dairy cattle and cat
670 affected with HPAI H5N1, we performed ISH and IHC on FFPE tissues as previously described[6]
671 Briefly, tissue sections were deparaffinized with xylene, washed with absolute ethanol, blocked
672 with peroxidase followed by antigen retrieval for one hour. For the ISH the V-InfluenzaA-H5N8-
673 M2M1 probe (Advanced Cell Diagnostics, Inc., Newark, CA) which targets H5Nx clade 2.3.4.4b
674 viruses and the RNAScope HD 2.5 assay were used as per manufacturer's instructions. ISH
675 signals were amplified with multiple amplifiers conjugated with alkaline phosphatase enzymes
676 and finally incubated with red substrate at room temperature for 10 minutes and counterstained
677 with hematoxylin. Immunohistochemistry was performed at the University of Georgia
678 Veterinary Diagnostic laboratory and the USDA-ARS Southeast Poultry Research Laboratory
679 following standard diagnostic IHC procedure. Specifically, tissue sections were treated with
680 Proteinase K for 5 min for antigen retrieval and incubated with monoclonal antibody (MAb)
681 against Influenza A virus M-protein (Meridian Bioscience, Catalog No. C65331M) at 1:100
682 dilution (UGA, VDL) or MAb against Influenza A NP (Clone 4F1; Southern Biotech Cat. No.:
683 10780-01) at 1:2000 dilution (SEPRL) for 1 hour. After washing the slides, the secondary
684 antibody anti-mouse IgG (Southern Biotech, cat 1070-04) at a 1:5000 dilution was added and

685 incubated with the slides for 1 h. All the slides were counterstained with hematoxylin, scanned at
686 40X resolution and the digital slides were examined for virus tropism and tissue distribution.

687 **Viral metagenomic sequencing:**

688 **Sample Collection and Processing:** Whole blood nasal swab samples were obtained from 10
689 cows from Farm 1 in Texas. Samples were submitted to the AHDC at Cornell University, on March
690 16, 2024. Upon receipt, metagenomic sequencing using the sequence-independent, single-primer
691 amplification (SISPA) procedure, the Oxford Nanopore sequencing chemistry and GridION
692 sequencing platform were performed as described below.

693 **Nucleic Acid (NA) Extraction, Library Preparation and Sequencing:** Nucleic acid (NA)
694 extraction was performed in 190 µl from each sample using the QIAamp MinElute Virus Spin Kit
695 (Qiagen). Prior to NA extraction samples were subjected to an enzymatic cocktail treatment
696 composed of 10X DNase 1 buffer, DNAse 1, Turbo DNAse, RNase Cocktail (ThermoFisher
697 Scientific), Baseline ZERO DNAse (Lucigen), Benzonase (Sigma-aldrich) and RNase ONE
698 Ribonuclease (Promega) to deplete host and bacterial nucleic acid. Purified NA was subjected to
699 SISPA, modified from a previously reported protocol [54] Briefly, 11 µL of nucleic acid was used in
700 a reverse transcription reaction with 100 pmol of primer FR20RV-12N (5'-
701 GCCGGAGCTCTGCAGATATCNNNNNNNNNNNN-3') using SuperScript IV reverse
702 transcriptase (Thermo Fisher Scientific), followed by second-strand synthesis using the Klenow
703 Fragment of DNA polymerase (NEB) with primer FR20RV-12N at 10 pmol. After purification
704 using Agencourt AMPure XP beads (Beckman Coulter), SISPA PCR amplification was conducted
705 with TaKaRa Taq DNA Polymerase (Takara) using the primer FR20RV (5'-
706 GCCGGAGCTCTGCAGATATC-3') at 10 pmol. SISPA products were converted into sequencing
707 libraries using the ligation sequencing kit (SQK-LSK109) and Native Barcoding Kit 96 V1 for

708 multiplex sequencing. Sequencing was performed on the FLO- MIN106 MinION flow cell r9.4.1
709 using the GridION Sequencer (Oxford Nanopore Technologies). A 24-hour sequencing run was
710 conducted, with fastq generation performed by the GridION using high accuracy base calling.
711 Settings were adjusted to accommodate barcodes at both ends and filter mid-strand barcodes. Fastq
712 reads were then filtered by size and quality using Nanofilt[55] and classified using Kraken version
713 2.1.0[56] followed by Bracken[57].

714 **Targeted Influenza A Sequencing**

715 Samples that tested positive for HPAI H5N1 and had Ct values <30 were subjected to targeted
716 influenza A sequencing at the Animal Health Diagnostic Center at Cornell University (Cornell
717 AHDC) and the Ohio Animal Disease Diagnostic Laboratory (Ohio ADDL). The set of 107
718 samples included samples from Farm 1, n=19; Farm 2, n=33; Farm 3, n=54; and Farm 7, n=1. A
719 complete metadata table with details on this set of samples is provided in **Supplementary Data**
720 **Table 1**. Initial targeted sequencing attempts on milk samples at Cornell AHDC utilizing high-
721 throughput diagnostic extraction methods[6], were unsuccessful in obtaining whole influenza A
722 genome sequences despite the utilization of samples with low cycle threshold (Ct) values. To
723 overcome this limitation up to 50 ml of each milk sample were pelleted at 1,770 x g for 15 min at
724 4ºC. The pellets were washed two times in PBS as described above and resuspended in 1 ml of
725 PBS-BSA. The resuspended pellet was then diluted 1:5 or 1:10 in PBS and 200 µl of this dilution
726 were used for extraction with the Indical IndiMag Pathogen kit (INDICAL Bioscience) on the
727 KingFisher Flex extractor (Thermo Fisher, Waltham, MA, USA). Whole influenza A virus genome
728 sequences were generated using the MBTuni-12 and MBtuni-13 M-RT-PCR methods[58].
729 Sequencing libraries were generated using the Native Barcoding Kit, EXP-NBD196, Ligation

730 Sequencing Kit, SQK-SQK109 (Oxford Nanopore Technologies [ONT]), and sequenced on a
731 FLO-MIN106 MinION flow cell r9.4.1 using the GriION platform.

732 Additionally, 31 samples from Farm 3 were subjected to target influenza A sequencing at
733 the OADDL using the Illumina DNA Prep Kit and the Nextera DNA CD Indexes. Paired-end
734 sequencing was performed on an Illumina MiSeq platform using the MiSeq Reagent Kit V3
735 (Illumina) with 2×250 base pair chemistry.

736 **Sequence analysis and mutational profiling**

737 Sequencing data generated by the GridION platform underwent high-accuracy basecalling and
738 demultiplexing of barcodes. Settings were configured to require barcodes at both ends and to
739 exclude reads with mid-read barcodes. The Nanofilt software version 2.8.0[55] was employed to
740 filter sequences based on quality thresholds. Reads with a quality score below 12 and those shorter
741 than 600 base pairs were removed from further analysis. Filtered reads were aligned to a reference
742 genome download from GenBank (A/Gallus/gallus_domesticus/Sonora/CPA-18486-
743 23/2023/H5N1, NCBI accession numbers OR801090.1 through OR801097.1) using Minialign
744 software version 0.4.4 (https://github.com/ocxtal/minialign). Consensus sequences were generated
745 using Medaka software version 1.4.3 with medaka_haploid_variant and medaka_consensus
746 programs for polishing (https://github.com/nanoporetech/medaka). Sequences with a read depth
747 greater than 20 and a quality score exceeding 20 were retained. Analysis of Illumina MiSeq data
748 was performed by trimming the reads with Trimmomatic version 0.39[59], and aligning, calling
749 variants and generating consensus sequences with Snippy version 4.6.0 (
750 https://github.com/tseemann/snippy). Genome sequences were annotated using Prokka software
751 version 1.14.5 to identify genetic features and functional elements[60]. The GenoFLU tool version
752 1.03 assessed potential reassortment events within the viral genome (https://github.com/USDA-

753 VS/GenoFLU). Genome alignments, mutations, SNPs, and annotation data were visualized using
754 Geneious Prime software (version 2024.0.). The FluSurver tool, available through GISAID EpiFlu,
755 was utilized to interpret the effects of mutations identified in the sequences, leveraging previously
756 published data (https://flusurver.bii.a-star.edu.sg/). Other mutation data was visualized using
757 protein consensus alignments in Geneious Prime software.

758 **Phylogenomic and Phylogeographic Analysis.**

759 The dataset consisted of HPAI H5N1 clade 2.3.4.4b genomes from samples collected between
760 January 2023 and March 2024 in the American continent, downloaded from GISAID Epiflu
761 database[33], and 91 complete genomes from the present study, that includes 50 genomes obtained
762 from raw sequencing data, combined with another 41 complete genomes curated from the GISAID
763 database that were obtained from the farms in our study (Farm 1, n=11; Farm 4, n=3; Farm 5, n=1;
764 Farm 6, n=4, Farm 7, n=5; Farm 8, n=6, and Farm 9, n=11). The genomes generated in this study
765 are deposited in GISAID database (**Supplementary Data Table 5),** and raw reads are available in
766 the Sequence Read Archive (SRA) under BioProject accession number PRJNA1114404.
767 Phylogenetic analyses were performed by using Augur v21.0.1 tool kit[61] procedures implemented
768 in Nextstrain[62]. Briefly, multiple sequence alignments were performed using MAFFT v7.515[63];
769 maximum likelihood trees were inferred using IQ-TREE v1.6.12[64] and the initial tree was refined
770 using sequence metadata through the augur refine subcommand. Discrete trait analysis was
771 performed using TreeTime v0.9.4[65]. The resultant dataset was visualized through Auspice.
772 Phylogenomic and phylogeographic analyses were also performed on complete genomes formed
773 by concatenation of all gene segments. Analyses were performed using Nextstrain as described
774 above, with the exception of the maximum-likelihood phylogenetic tree inferred using IQ-tree with
775 an edge-linked partition model and 1000 bootstrap replicates. The potential transmission networks

776 between farms were inferred using the PB2 gene sequences in PopART package v1.7.2 using
777 median joining tree method with an epsilon of zero[66].

778 **Reassortment and MRCA identification**
779
780 All the type A influenza sequences (n = 3620, North America) from avian, dairy cattle, and other
781 mammals between January 2020 and May 2024 were downloaded from Epiflu database in
782 GISAID[33]. Only complete gene fragments were used to infer maximum likelihood phylogenetic
783 trees for each fragment using IQ-TREE with generalized time-reversible (GTR) nucleotide
784 substitutions model[64]. The HA phylogeny was used to identify the reassortment events using
785 TreeSort v.0.1.1 (maximum molecular clock deviation parameter of 2.5) (https://github.com/flu-
786 crew/TreeSort). We implemented Bayesian Evolutionary Analysis Sampling Tree (BEAST,
787 V1.10) framework with BEAGLE library v4.0.1 to estimate the MRCA for the individual gene
788 fragments (GTR gamma distributed site heterogeneity model, strict clock model, three independent
789 Markov chain Monte Carlo (MCMC) sampling runs with 10 million iterations with sampling every
790 10,000 iterations[67]. Tracer V1.7.2[68] was used to analyze the results. The maximum clade credibility
791 tree was generated using TreeAnnotator V1.8.4 using median node heights and 10 percent burn-
792 in[67] and visualized with FigTree (V1.4.4) (http://tree.bio.ed.ac.uk/software/figtree/).

793
794 **Methods references**

795 51. Centers for Disease Control and Prevention. CDC Confirms Second Human H5 Bird Flu
796 Case in Michigan, Third Case Tied to Dairy Outbreak | CDC Online Newsroom | CDC.
797 https://www.cdc.gov/media/releases/2024/p0530-h5-human-case-michigan.html.
798 52. Garg, S. *et al.* Outbreak of Highly Pathogenic Avian Influenza A (H5N1) Viruses in U .
799 S . Dairy Cattle and Detection of Two Human Cases — United States , 2024. *CDC -*
800 *Morb. Mortal. Wkly. Rep.* **73**, (2024).
801 53. The National Animal Health Laboratory Network. Standard operating procedure for real-
802 time RT-PCR detection of influenza A and avian paramyxovirus type-1 (NVSL-SOP-
803 0068). https://www.aphis.usda.gov/media/document/15399/file (2023).
804 54. Chrzastek, K. *et al.* Use of Sequence-Independent, Single-Primer-Amplification (SISPA)
805 for rapid detection, identification, and characterization of avian RNA viruses. *Virology*
806 **509**, 159–166 (2017).

55. De Coster, W., D'Hert, S., Schultz, D. T., Cruts, M. & Van Broeckhoven, C. NanoPack: visualizing and processing long-read sequencing data. *Bioinformatics* **34**, 2666–2669 (2018).
56. Wood, D. E., Lu, J. & Langmead, B. Improved metagenomic analysis with Kraken 2. *Genome Biol.* **20**, 257 (2019).
57. Lu, J. *et al.* Metagenome analysis using the Kraken software suite. *Nat. Protoc.* **17**, 2815–2839 (2022).
58. Mitchell, P. K. *et al.* Method comparison of targeted influenza A virus typing and whole-genome sequencing from respiratory specimens of companion animals. *J. Vet. Diagnostic Investig.* **33**, 191–201 (2021).
59. Bolger, A. M., Lohse, M. & Usadel, B. Trimmomatic: a flexible trimmer for Illumina sequence data. *Bioinformatics* **30**, 2114–2120 (2014).
60. Seemann, T. Prokka: rapid prokaryotic genome annotation. *Bioinformatics* **30**, 2068–2069 (2014).
61. Huddleston, J. *et al.* Augur: a bioinformatics toolkit for phylogenetic analyses of human pathogens. *J. open source Softw.* **6**, (2021).
62. Hadfield, J. *et al.* NextStrain: Real-time tracking of pathogen evolution. *Bioinformatics* **34**, 4121–4123 (2018).
63. Katoh, K. & Standley, D. M. MAFFT multiple sequence alignment software version 7: Improvements in performance and usability. *Mol. Biol. Evol.* **30**, 772–780 (2013).
64. Minh, B. Q. *et al.* IQ-TREE 2: New Models and Efficient Methods for Phylogenetic Inference in the Genomic Era. *Mol. Biol. Evol.* **37**, 1530–1534 (2020).
65. Sagulenko, P., Puller, V. & Neher, R. A. TreeTime: Maximum-likelihood phylodynamic analysis. *Virus Evol.* **4**, vex042 (2018).
66. Leigh, J. W. & Bryant, D. POPART: full-feature software for haplotype network construction. (2015) doi:10.1111/2041-210X.12410.
67. Suchard, M. A. *et al.* Bayesian phylogenetic and phylodynamic data integration using BEAST 1.10. *Virus Evol.* **4**, vey016 (2018).
68. Rambaut, A., Drummond, A. J., Xie, D., Baele, G. & Suchard, M. A. Posterior Summarization in Bayesian Phylogenetics Using Tracer 1.7. *Syst. Biol.* **67**, 901–904 (2018).

Acknowledgements

The authors would like to thank the producers and veterinarians who submitted samples and contributed for this investigation. The work was funded by the AHDC, OADDL and TVMDL. This work was supported in part by USDA-NIFA grant no. 2021-68014-33635 (D.G.D, K.D.) and APHIS NALHN Enhancement grant no. AP21VSD&B000C005 (K.D., D.G.D). We gratefully acknowledge all data contributors including the authors and their originating laboratories

responsible for obtaining the specimens, and their submitting laboratories for generating the genetic sequence and metadata and sharing via the GISAID initiative. The artwork in Fig. 6 and Extended Data Fig. 5 and the panels of Fig. 3, Extended Data Fig. 2, Extended Data Fig. 3 and Extended Data Fig. 4 were created with Biorender.com.

Author contribution

Conceptualization: DGD; Methodology: EF, SLB, ML, MN, LC, ACT, MPK, BC, AJ, KK, ED, GG, GH, MM, ERA, TH; Software: LCC, BK; Validation: SLB, ML, MN, LC, MPK, BC, AJ; Formal analysis: LCC, SLB, ML, BC, DGD; Investigation: LCC, EF, SLB, ML, LC, ACT, MPK, BC, AJ, DRK, MM, ERA; Resources: EF, ACT, DLS, ML, AS, FE, KD, DGD; Data Curation: LCC, EF, SLB, ML, KD, DGD; Writing - Original Draft: LCC, SLB, BK, DGD; Writing - Review & Editing: LCC, EF, SLB, ML, MN, LC, ACT, MPK, BC, AJ, KK, ED, GG, GH, MM, DRK, DLS, ERA, TH, MLV, AS, FE, KD, DGD; Visualization: LCC, SLB, BC, DGD; Supervision: DGD; Project administration: MPK, KD, DGD, Funding acquisition: AS, FE, KD, DGD.

Competing interest

The authors declare no competing interests.

Additional information

Supplementary information The online version contains supplementary material available at:

Correspondence and requests for materials should be addressed to D.G. Diel.

Peer review information Nature thanks XX and the other, anonymous, reviewer(s) for their contribution to the peer review of this work. Peer reviewer reports are available.

Data availability

All HPAI H5N1 virus sequences generated in this study are deposited in GISAID (https:www.gisaid.org/; accession numbers are available in Supplementary Data Table 5), and raw reads have been deposited in NCBI's Short Read Archive (BioProject number PRJNA1114404). All additional influenza sequences used in our analysis were obtained from GISAID (accession numbers available in Supplementary Data Table 4), or NCBI nucleotide (https://www.ncbi.nlm.nih.gov/nucleotide/).

Extended Data Figure Legends

Extended Data Fig. 1 | Clinical presentation of HPAI H5N1 infection in dairy cattle. a, Clinically affected animals presenting clear nasal discharge and involution of the mammary gland/udder (gold arrowheads, top images) and depression (bottom images). **b**, Milk from HPAI H5N1 infected animals presenting yellowish colostrum-like color and appearance (top panels) or coloration varying from yellowish to pink/brown color. Curdling of milk visible in some samples.

902 **Extended Data Fig. 2 | Highly pathogenic avian influenza H5N1 virus detection in cat tissues.**
903 Hematoxylin and eosin (H&E) staining (left panels) showing; **a**, multifocal area of perivascular
904 cuffing, vascular congestion, and perivascular edema (Z0), neuronal swelling and neuronal
905 necrosis and perivascular edema in brain (Z1, Z2 and Z3). **b**, pulmonary edema with strands
906 of fibrin, thickened alveolar septa and intraepithelial lymphocytes, alveolar capillary congestion.
907 **c**, single cell necrosis and hemorrhage in liver. In situ hybridization (ISH) (middle panels) targeting
908 Influenza A virus (Matrix gene) showing (**a)** multifocal areas with extensive viral RNA (Z0), in
909 neurons and glial cells within the granular layer and nuclear and intracytoplasmic viral RNA in
910 neuronal soma, axon, and vascular endothelial cells in brain (Z1, Z2 and Z3), **b**, viral RNA in
911 bronchiolar epithelial cells and type II pneumocytes, and **c**, viral RNA in resident sinusoidal
912 Kupffer cells and vascular endothelial cells. Immunohistochemistry (IHC) (right panels) targeting
913 Influenza A virus M gene showing immunolabeling of (**a**) multifocal areas of
914 immunolabeling (Z0), intracytoplasmic immunolabeling of viral antigen in neuronal soma and
915 axons within granular layer in brain (Z1, Z2 and Z3), **b**, bronchiolar epithelial cells and type II
916 pneumocytes in lung, and **c**, vascular endothelial cells and resident sinusoidal Kupffer cells.
917 Tissues from one cat were available and subjected to histological, ISH and IHC analysis.
918 **Extended Data Fig. 3 | Highly pathogenic avian influenza H5N1 virus RNA detection in**
919 **cow tissues.** In situ hybridization of viral RNA in mononuclear cells of lymphoid follicles in
920 lymph node, mononuclear cells of bronchial associated lymphoid tissue (BALT) in the lung,
921 endothelial cells of blood vessels in the heart, endothelial cells of blood vessels in the colon,
922 mononuclear cells in the spleen and endothelial cells and resident sinusoidal Kupffer cells in the
923 liver. The zoom in (Z1) represents the demarcated area in the left panels (Z0). Tissues from three
924 cows were available and subjected to histological, ISH and IHC analysis.

925

926 **Extended Data Fig. 4 | Highly pathogenic avian influenza H5N1 virus antigen detection in**
927 **cow tissues.** Immunohistochemical staining of viral antigen in mononuclear cells of lymphoid
928 follicles in lymph node, mononuclear cells of bronchial associated lymphoid tissue (BALT) in the
929 lung, endothelial cells of blood vessels in the heart, endothelial cells of blood vessels in the colon,
930 mononuclear cells in the spleen and endothelial cells and resident sinusoidal Kupffer cells in the
931 liver. The zoom in (Z1) represents the demarcated area in the left panels (Z0). Tissues from three
932 cows were available and subjected to histological, ISH and IHC analysis.

933

934 **Extended Data Fig. 5 | Bayesian analysis and estimation of reassortment events leading to**
935 **emergence of HPAI H5N1 virus clade 2.3.4.4b genotype B3.13.** Estimation of tMRCA and
936 immediate descendants of MRCA donors of PB2 (**a**), PB1 (**b**), NP (**c**) and NS (**d**) genes,
937 respectively. **e**, Reassortment event of PB2 and NP which lead to emergence of genotype 3.13 in
938 an unknown host before detection in skunk, avian species, and dairy cattle. The teal color of
939 branches indicates the reassortment event.

940

941 **Extended Data Fig. 6 | Phylogenetic analysis of HPAI H5N1 viruses.** Phylogenetic trees
942 constructed with each influenza A virus genome segment, comprising 91 sequences of samples
943 described in this study and 648 sequences of samples collected throughout the American
944 continent, collected between January 2023 and March 2024, available at the
945 GISAID EpiFlu database.

946

947 **Extended data Fig. 7 | Wild bird sequences HPAI H5N1 are related to sequences from cows**
948 **in affected dairy farms. a**, Genetic relationship of HPAI H5N1 sequences recovered from

949 blackbirds with sequences recovered from cattle in Farms 7 and 9. Nodes are colored by premise
950 and all the samples collected in the referred farm are highlighted. **b**, Detailed/zoom in view of the
951 sequence clusters containing samples from Farm 7, Farm 9 and sequences from blackbirds
952 collected at 8-12 Km from Farm 7. Analysis was conducted based on whole concatenated genome
953 sequences.
954
955 **Extended Data Fig. 8 | Evidence of interspecies transmission of HPAI H5N1. a,** Close
956 phylogenetic relationship between HPAI H5N1 sequences recovered from dairy cows, great-tailed
957 grackles, and cat in Farm 1. **b**, Close phylogenetic relationship between HPAI H5N1 sequences
958 recovered from dairy cows and a racoon in Farm 8. Nodes are colored by host and all the samples
959 collected in the specific farm are highlighted. Panels on the right are a detailed view of the clusters
960 containing more than one host species. Analysis was conducted based on whole concatenated
961 genome sequences.
962
963 **Extended Data Table Titles and Footnotes**
964
965 **Extended Data Table 1 | Summary of clinical investigation on HPAI affected farms.**
966 [a]Number of cows clinically affected in each farm during the outbreak. The proportion of affected
967 animals over the total number of cows in the farm/herd is presented as percentage in parenthesis.
968 **Additional notes**; Farm 1 (TX1) shipped 42 apparently healthy lactating cows (based on official
969 pre-movement Certificate of Veterinary Inspection) to Farm 3 (OH1) on 03/07/24. Cats and birds
970 in Farm 1 died after the outbreak in cattle. Cats were fed raw milk; Farm 3 (OH1): Received 42
971 apparently healthy lactating cows (based on official pre-movement Certificate of Veterinary
972 Inspection) from Farm 1 (TX1) on 03/08/24, Cats were not tested for HPAI but died after the

973 outbreak in cattle; Farm 4 (NM1): Cats died after the outbreak in cattle; Farm 5 (TX3): Cats died
974 after the outbreak in cattle; Farm 8 (NM2): Wild birds, cats and racoon died after the outbreak in
975 cattle.
976
977 **Extended Data Table 2 | Viral RNA loads (Ct values) in samples from HPAI affected animals**
978 **in a farm.**
979 Note: NEG, Negative; -, Not tested
980
981 **Extended Data Table 3 | Virus detection by *in situ* hybridization and immunohistochemistry**
982 **in cattle and cat tissues.**
983 Note: -: negative; +: weak positive; ++: moderate positive at multiple locations; +++: strong
984 positive at multiple locations; N/T: not tested; GALT: gut associated lymphoid tissue; BALT:
985 bronchus associated lymphoid tissue.
986
987 **Extended Data Table 4 | Reticulate evolution of genome fragments of HPAI H5N1 clade**
988 **2.3.4.4b genotype B3.13**.
989 Note: N/A: Unassigned genotype, --: unassigned lineage by GenoFlu. Grey colored row is an
990 unknow host in which reassortant genotype B3.13 was originated. The light blue color shows ea1
991 lineage of PA, HA, NA, and M genes. Green, brown, pink, and purple colors show NS, PB2, PB1
992 and NP genes originated and evolved from different HA and NA types of avian influenza virus
993 and finally identified in currently circulating genotype B3.13. [A]EPI_ISL_16215525,
994 [B]EPI_ISL_6795387, [C]EPI_ISL_12968823, [D]EPI_ISL_18133029, [E]EPI_ISL_18665478,
995 [F]EPI_ISL_16215781, [G]EPI_ISL_17260689, [H]EPI_ISL_17424646, [I]EPI_ISL_18741779,

996 [J]EPI_ISL_19064382, [K]EPI_ISL_18737538, [L]EPI_ISL_19064368, [M]EPI_ISL_19014396,
997 [N]EPI_ISL_19014398, [O]EPI_ISL_19014400, [P]EPI_ISL_19014404, [Q]EPI_ISL_19094493,
998 [R]EPI_ISL_19094764, [S]EPI_ISL_19027114.
999
1000 **Extended Data Table 5 | Comparative mutational spectrum of H5N1 clade 2.3.4.4b genotypes**
1001 **in different host species from 2021-2024.**
1002 Note: A/chicken/NL/FAV-0033/2021|2021-12-21|2.3.4.4b was used as reference [first sequence
1003 detected in North America (Canada)]. -; gene fragment not available. All sequences used in the
1004 analysis are provided in supplementary data table 4. All the cattle HPAI H5N1 genotype B3.13
1005 variants with <1% frequency are shown in the supplementary data table 6.
1006 The superscripts are abbreviation of species; BV: black vulture, CG: Canada goose, Ck: chicken,
1007 Co: cormorant, CR: crow, E: eagle, ER: eared grebe, F: falcon, G: goose, GHO: great horn own,
1008 PC: peacock, RTH: red tail hawk, SG: snow goose, Tk: turkey, TV: turkey vulture, WD: wood
1009 duck, WS: western screech, MS: multiple species, Ph: pheasant, *: polymorphism, TX; Texas, MI:
1010 Michigan.
1011 Highlighted rows colors; Light blue: mutation specific to HPAI H5N1 Clade 2.3.4.4b genotype
1012 B3.13, Pink: cattle variants with frequency above 5%, Green: mutations emerged in 2023 and
1013 circulated in cattle sequences in 2024, Brown: mutations in Human or human, falcon, and skunk
1014 sequences in 2024, Grey: virus adaptation mutation to mammalian hosts.
1015
1016
1017 **Extended Data Table 6 | Extended data table 6. Microscopic changes in tissues from cattle and**
1018 **cat.**
1019 Note: -: negative detection; +: presence of microscopic changes; N/T: tissues not tested.

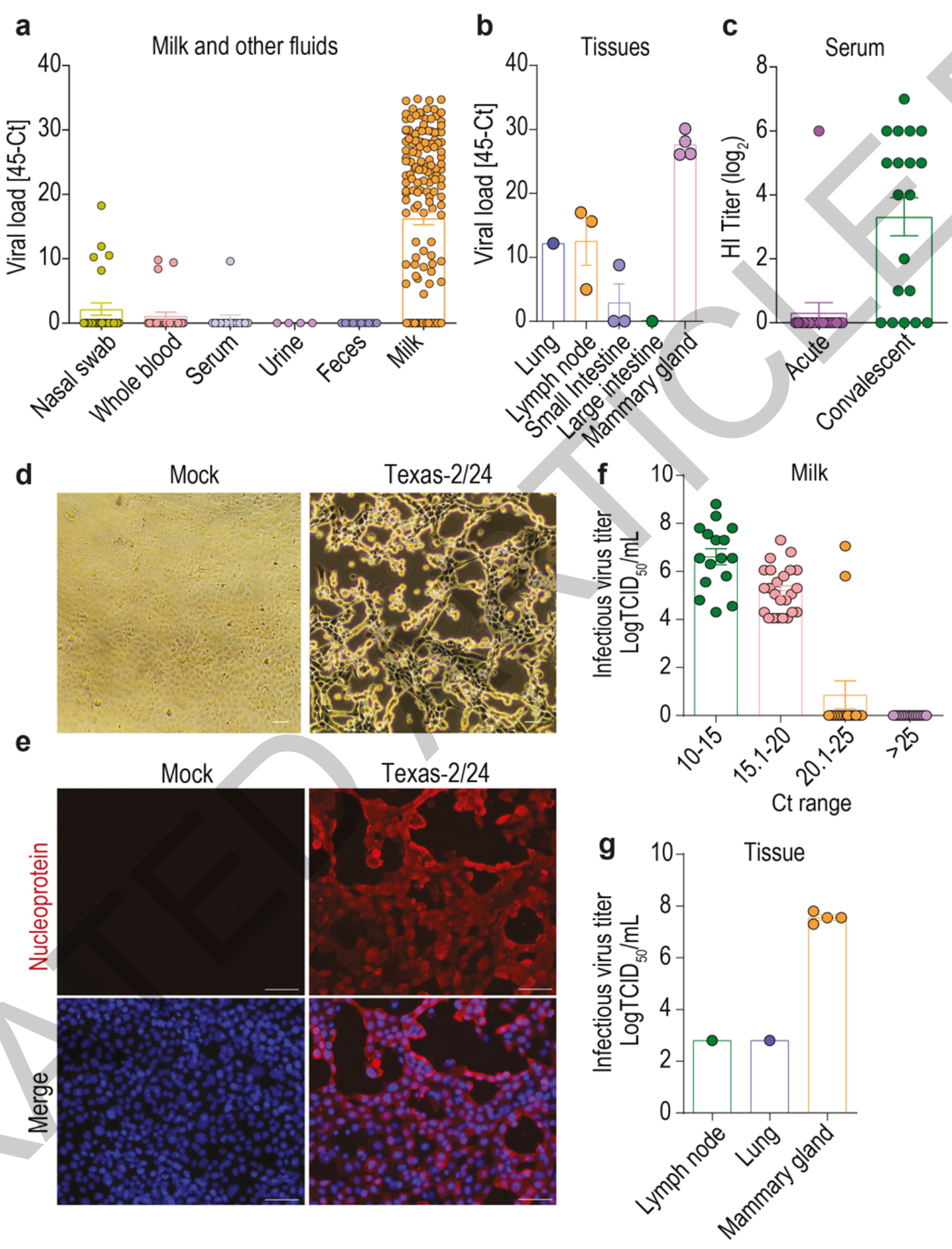
a
Milk and other fluids
Viral load [45-Ct]
40
30
20
10
0
Nasal swab
Whole blood
Serum
Urine
Feces
Milk
b
Tissues
Viral load [45-Ct]
Lung
Lymph node
Small Intestine
Large intestine
Mammary gland
c
Serum
HI Titer (log2)
8
6
4
2
0
Acute
Convalescent
d
Mock
Texas-2/24
e
Mock
Texas-2/24
Nucleoprotein
Merge
f
Milk
Infectious virus titer LogTCID50/mL
10
8
6
4
2
0
10-15
15.1-20
20.1-25
>25
Ct range
g
Tissue
Infectious virus titer LogTCID50/mL
Lymph node
Lung
Mammary gland

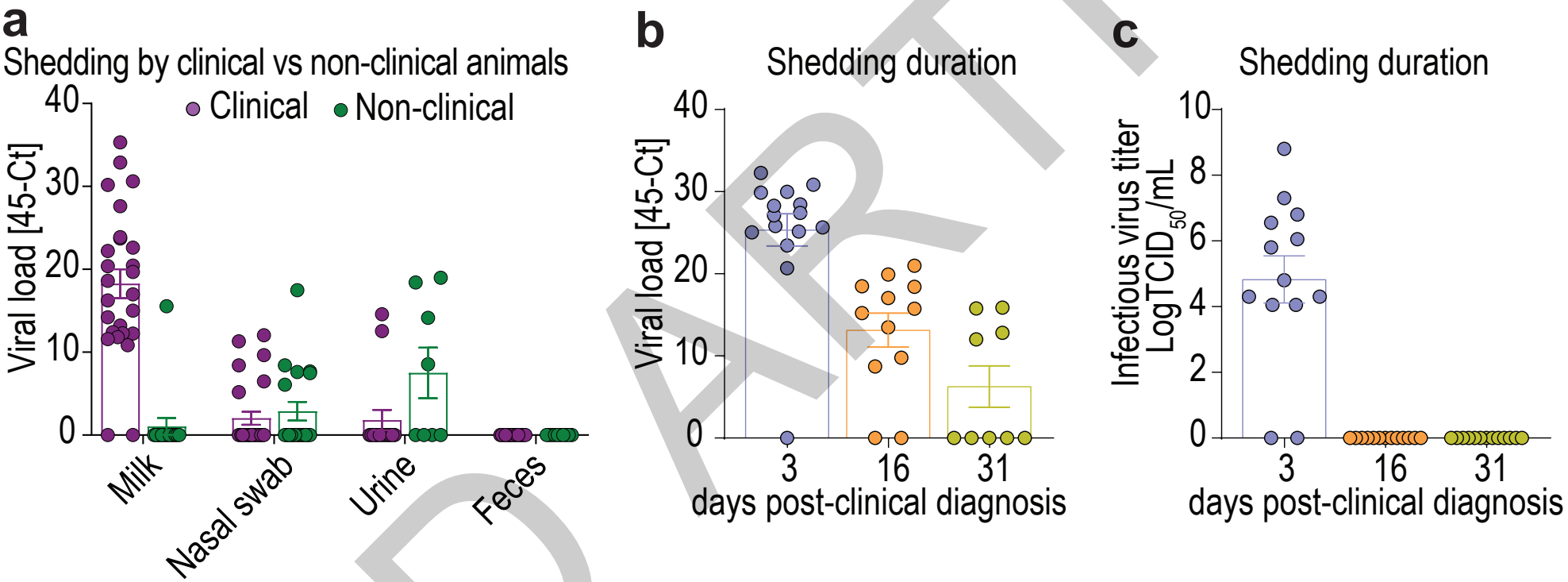
a
Shedding by clinical vs non-clinical animals
Clinical
Non-clinical
Viral load [45-Ct]
40
30
20
10
0
Milk
Nasal swab
Urine
Feces
b
Shedding duration
Viral load [45-Ct]
40
30
20
10
0
3
16
31
days post-clinical diagnosis
c
Shedding duration
Infectious virus titer
LogTCID50/mL
10
8
6
4
2
0
3
16
31
days post-clinical diagnosis

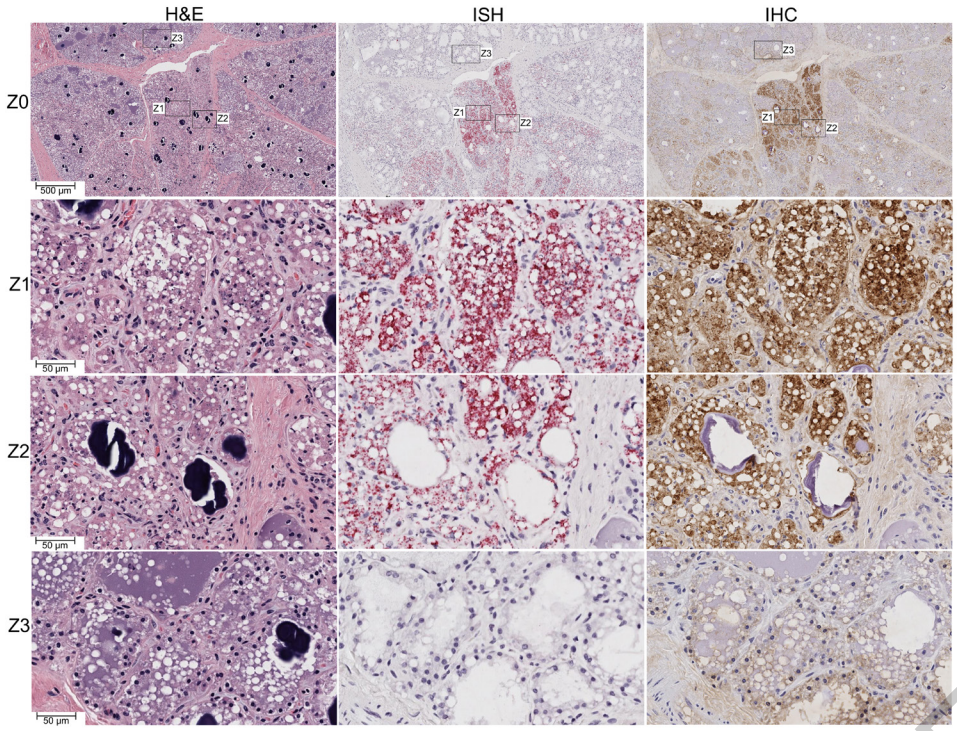

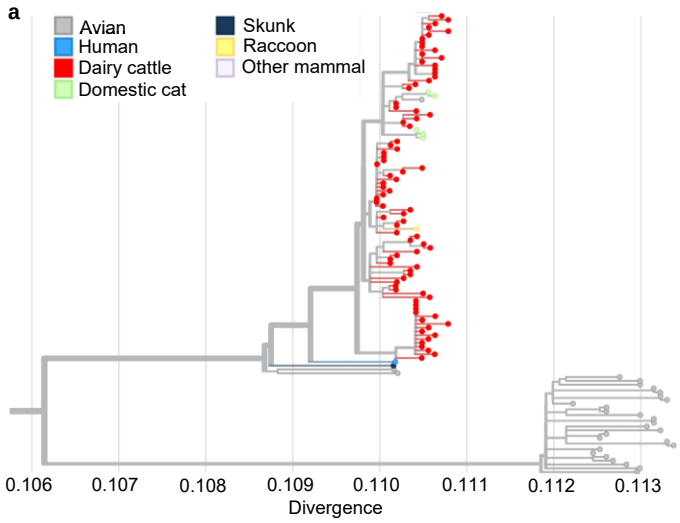

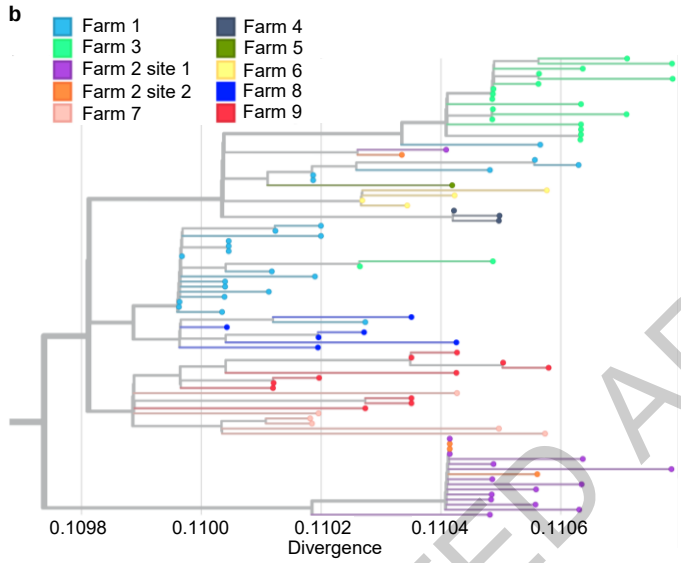

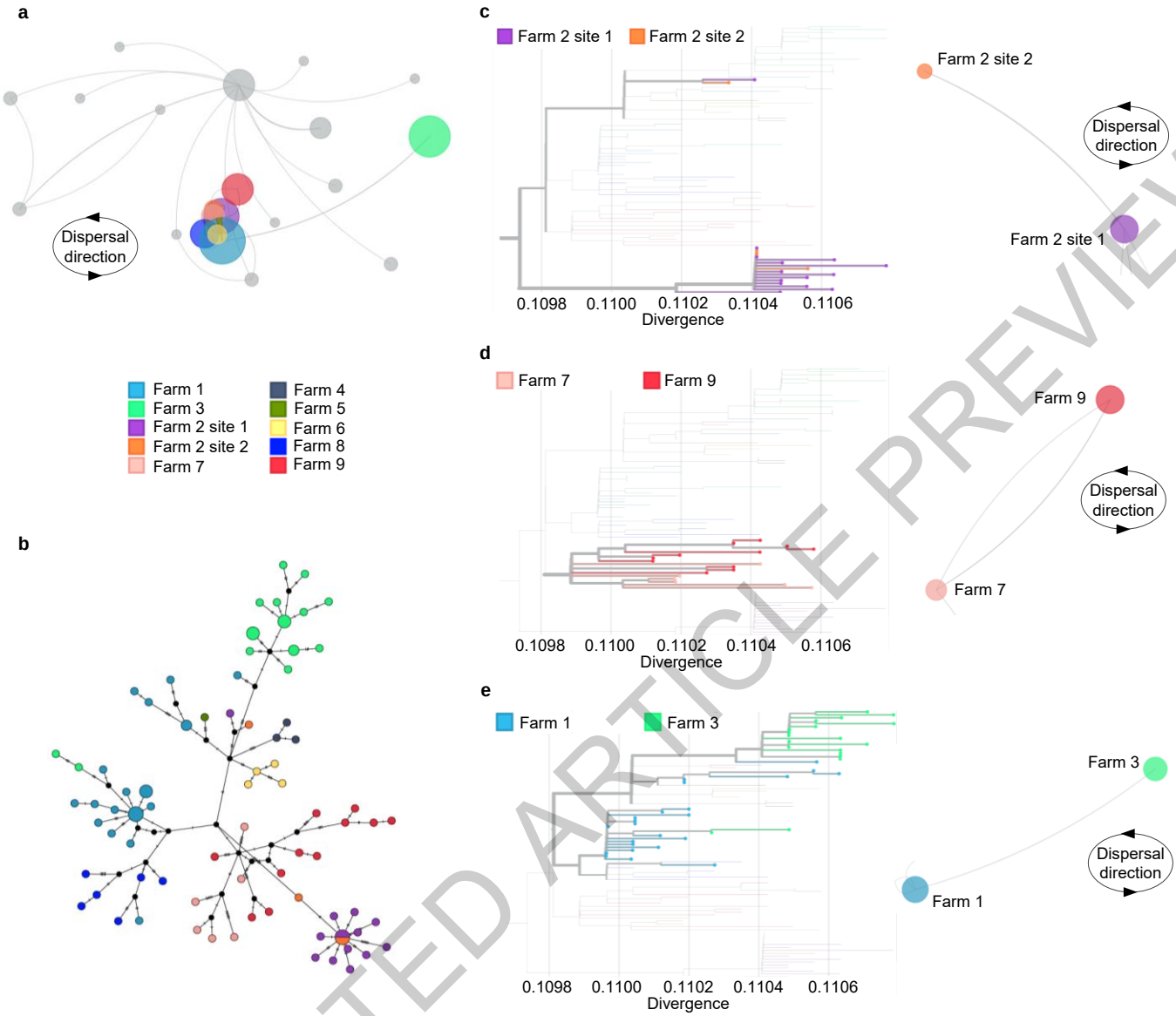

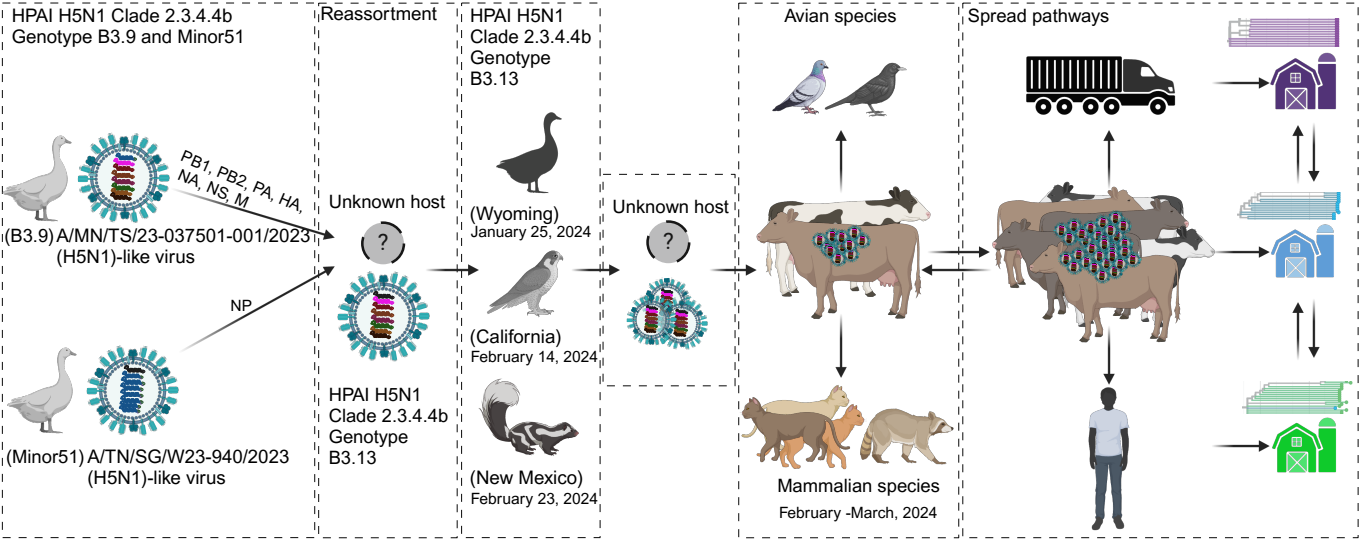
HPAI H5N1 Clade 2.3.4.4b
Genotype B3.9 and Minor51
PB1, PB2, PA, HA, NA, NS, M
(B3.9) A/MN/TS/23-037501-001/2023
(H5N1)-like virus
NP
(Minor51) A/TN/SG/W23-940/2023
(H5N1)-like virus
Reassortment
Unknown host
?
HPAI H5N1
Clade 2.3.4.4b
Genotype
B3.13
HPAI H5N1
Clade 2.3.4.4b
Genotype
B3.13
(Wyoming)
January 25, 2024
(California)
February 14, 2024
(New Mexico)
February 23, 2024
Unknown host
?
Avian species
Mammalian species
February -March, 2024
Spread pathways

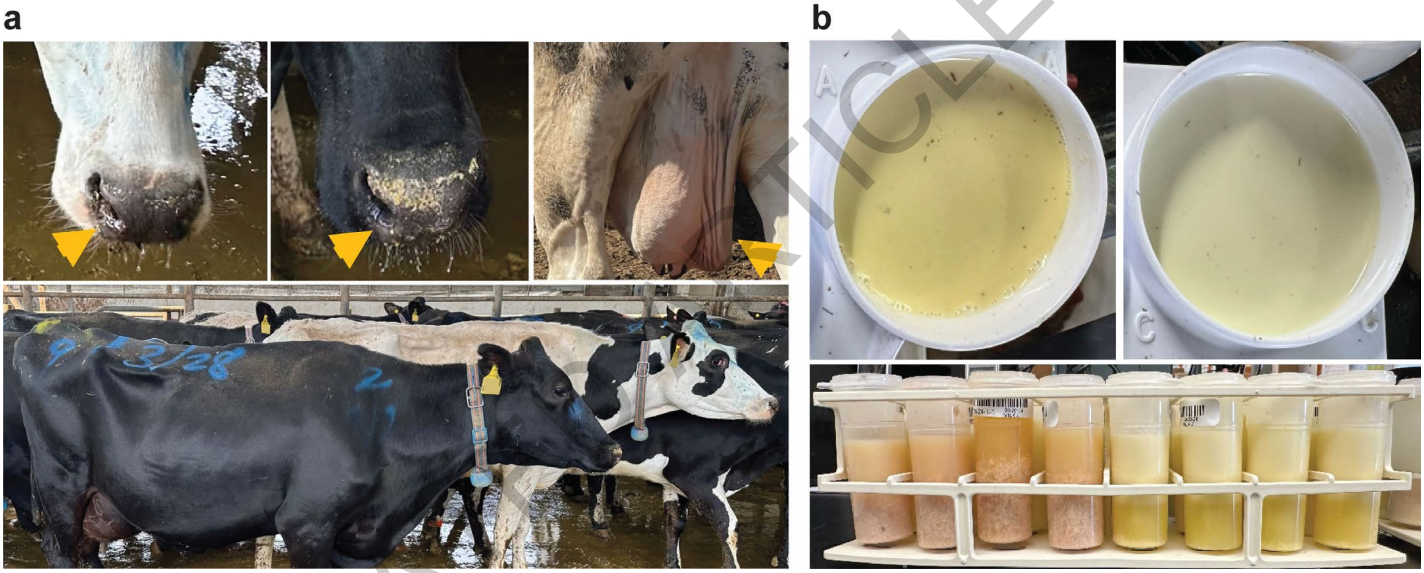

Extended Data Fig. 1

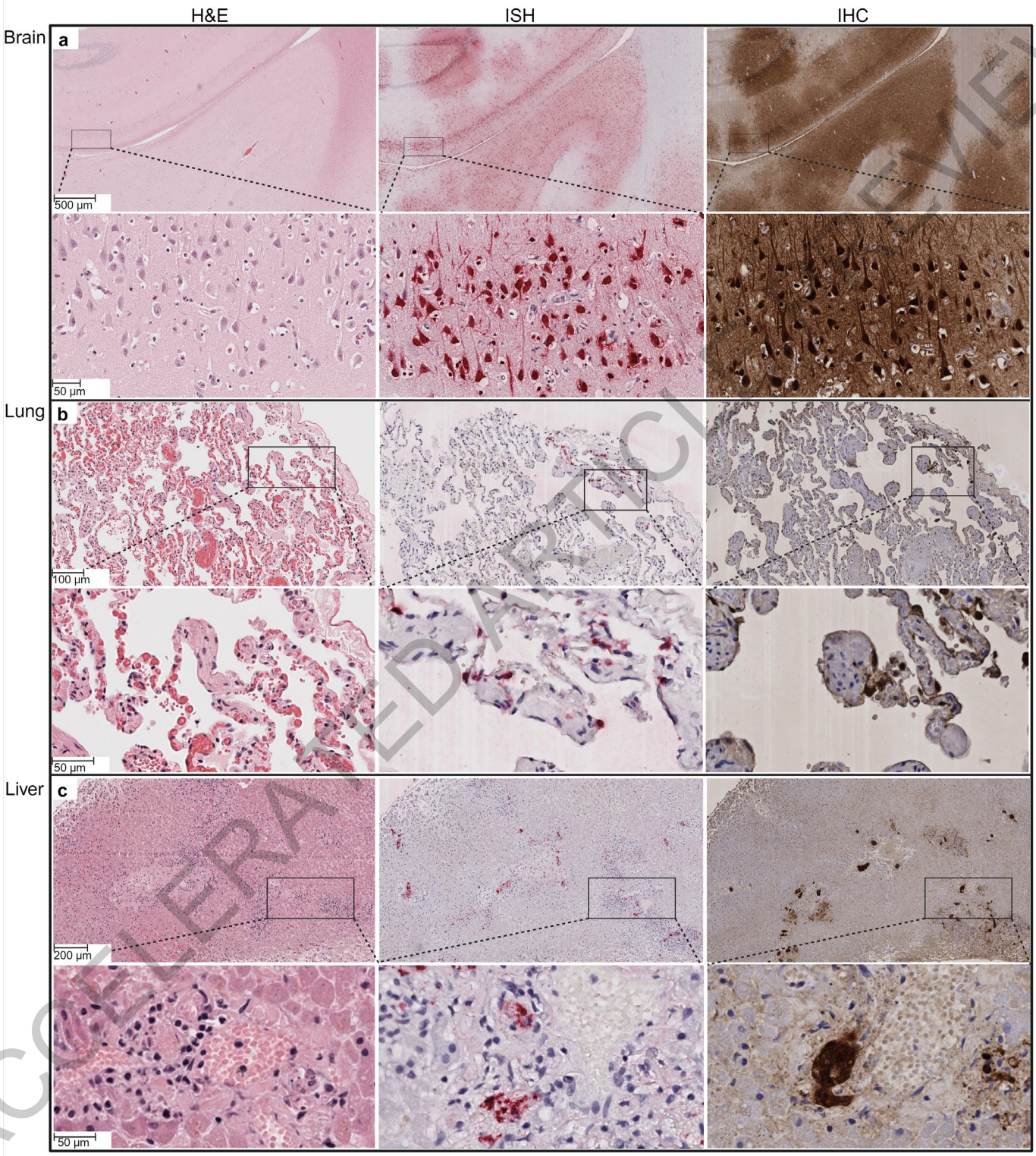

Extended Data Fig. 2

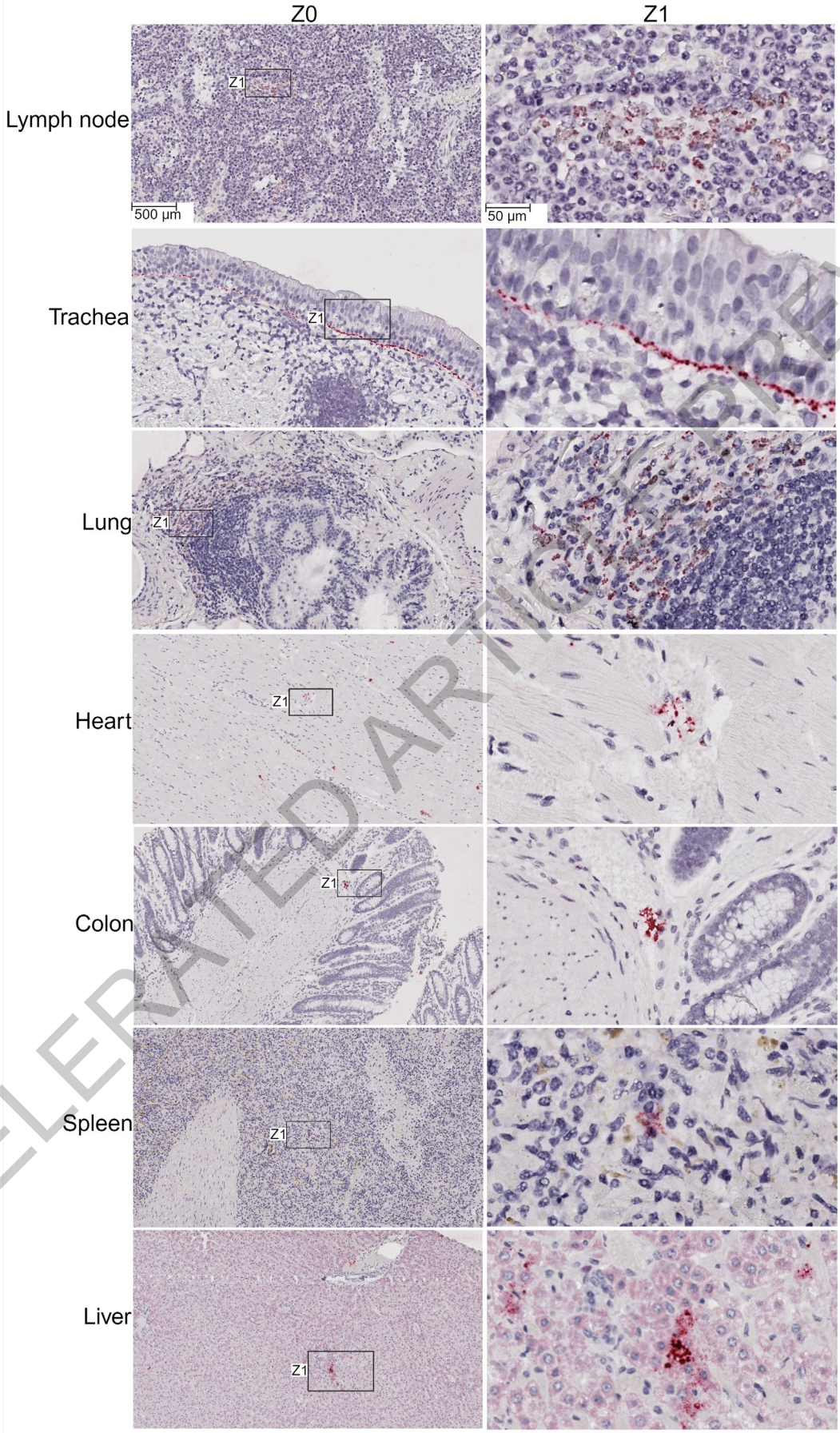

Extended Data Fig. 3

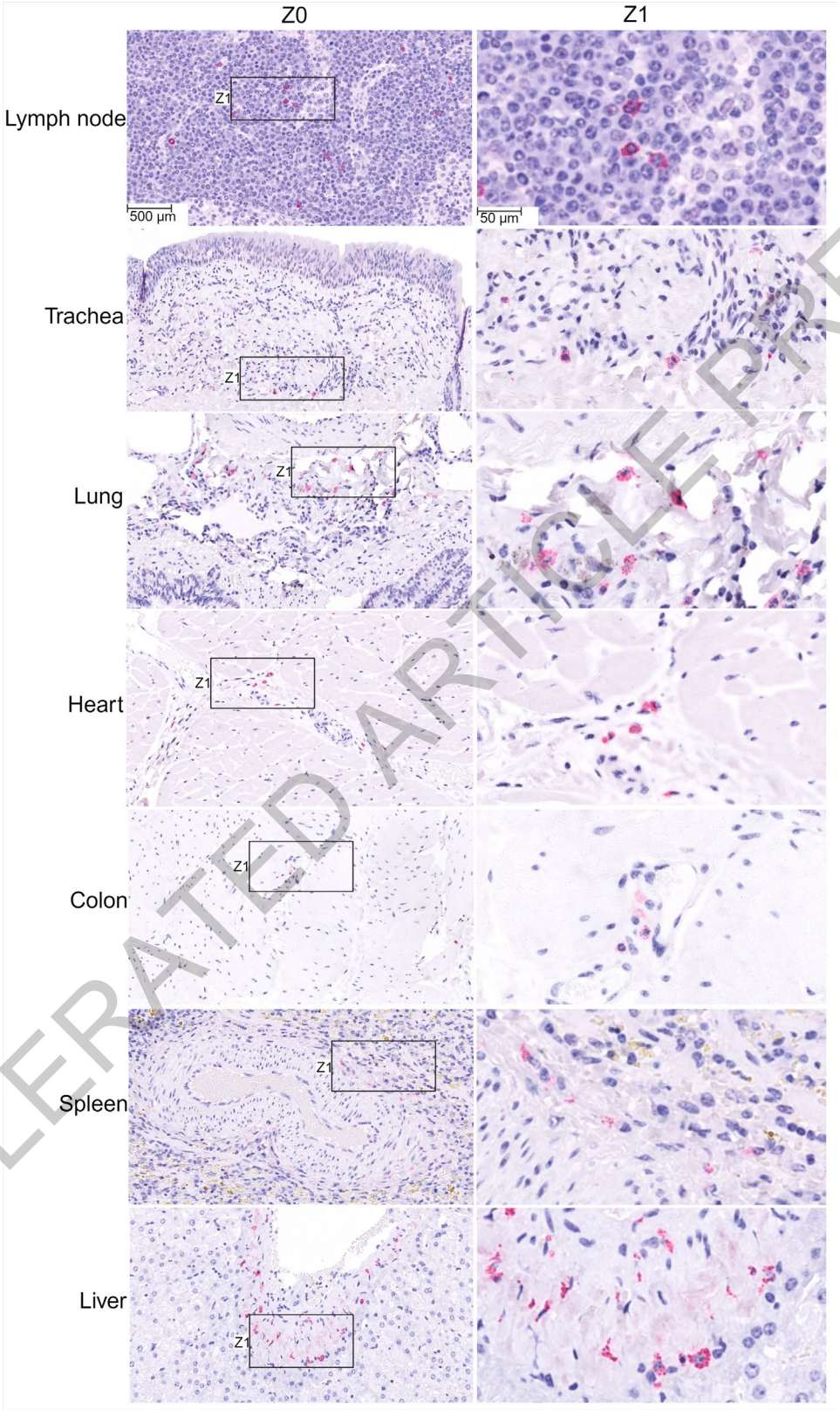

Extended Data Fig. 4

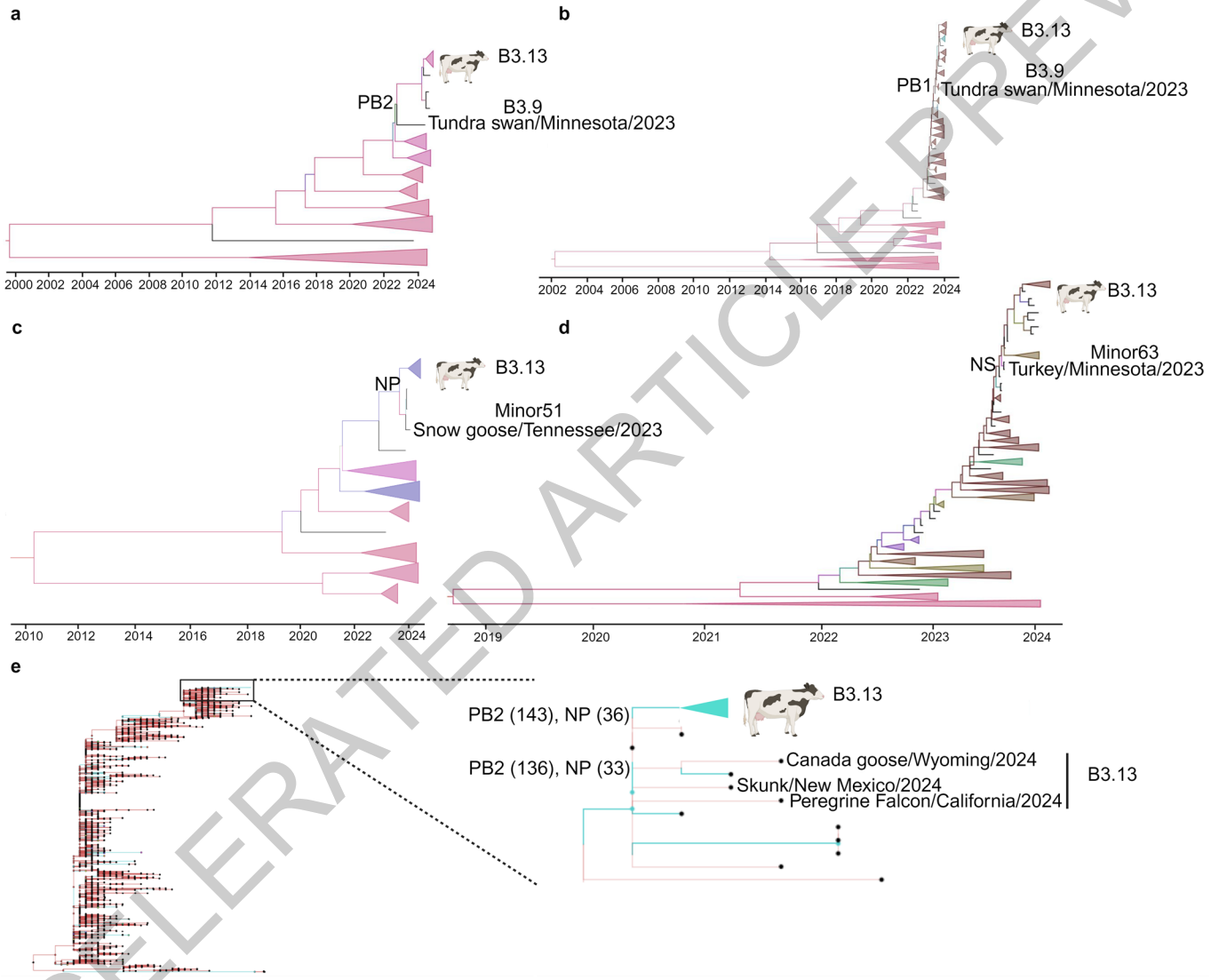

Extended Data Fig. 5

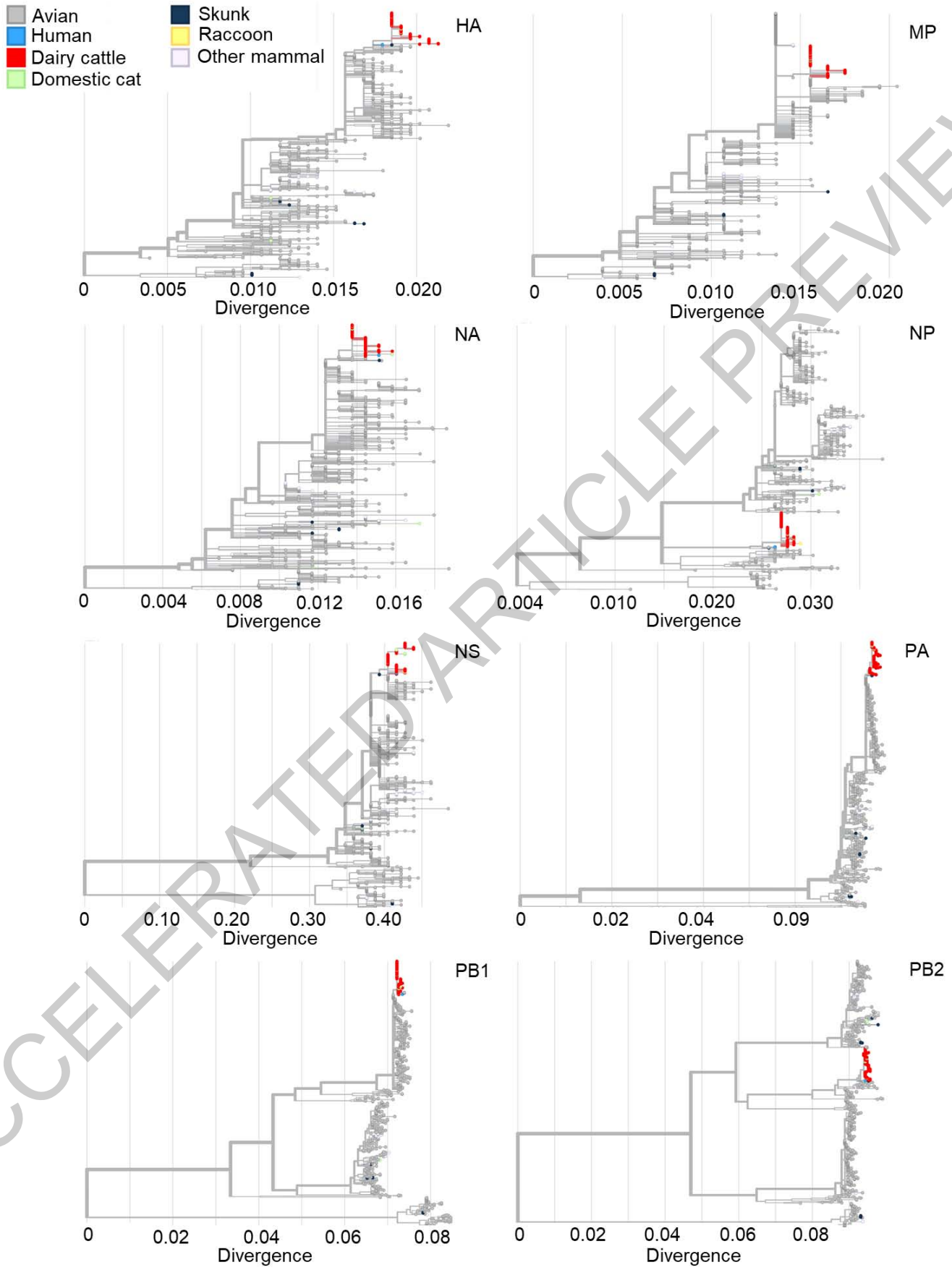

Extended Data Fig. 6

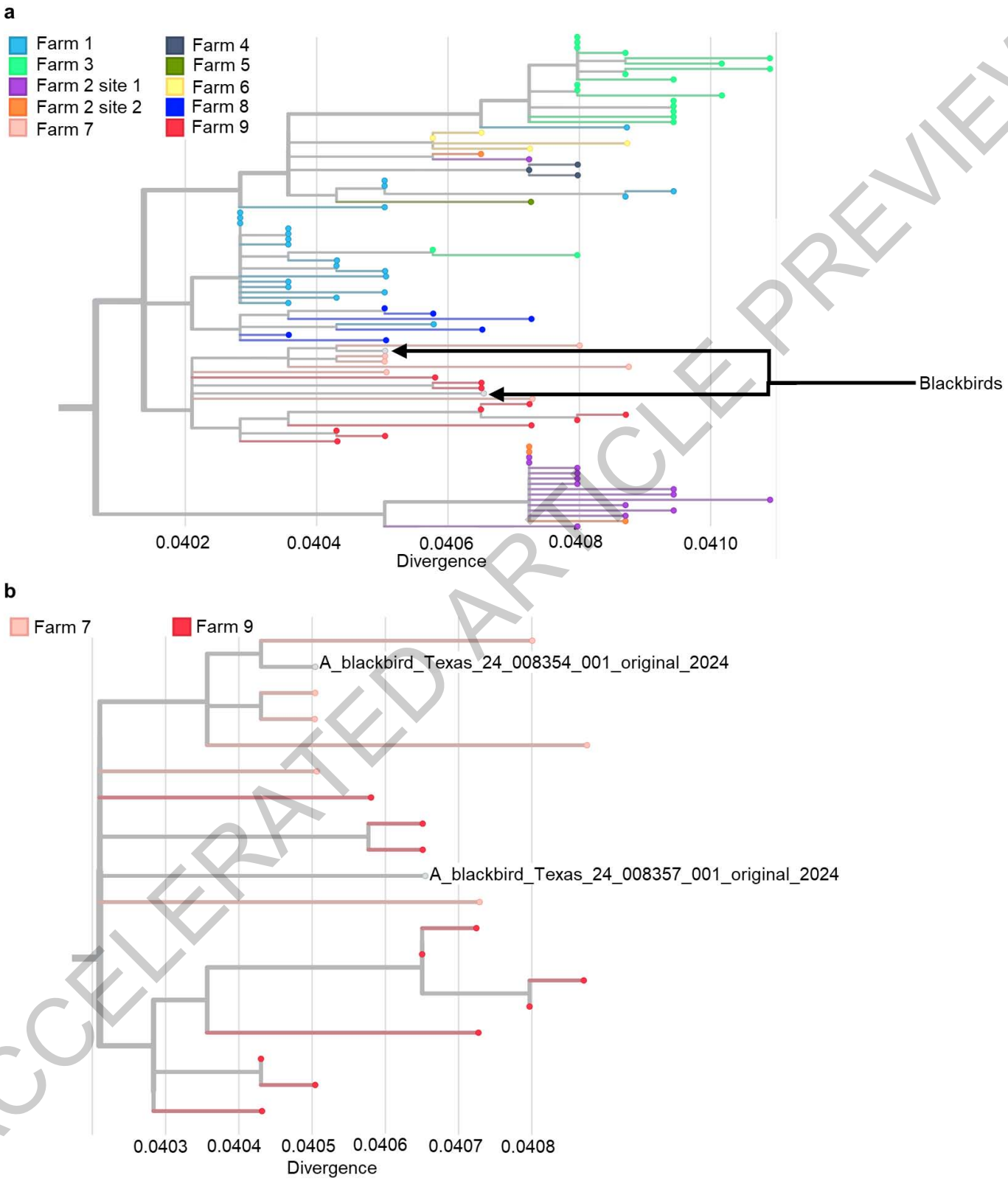

Extended Data Fig. 7

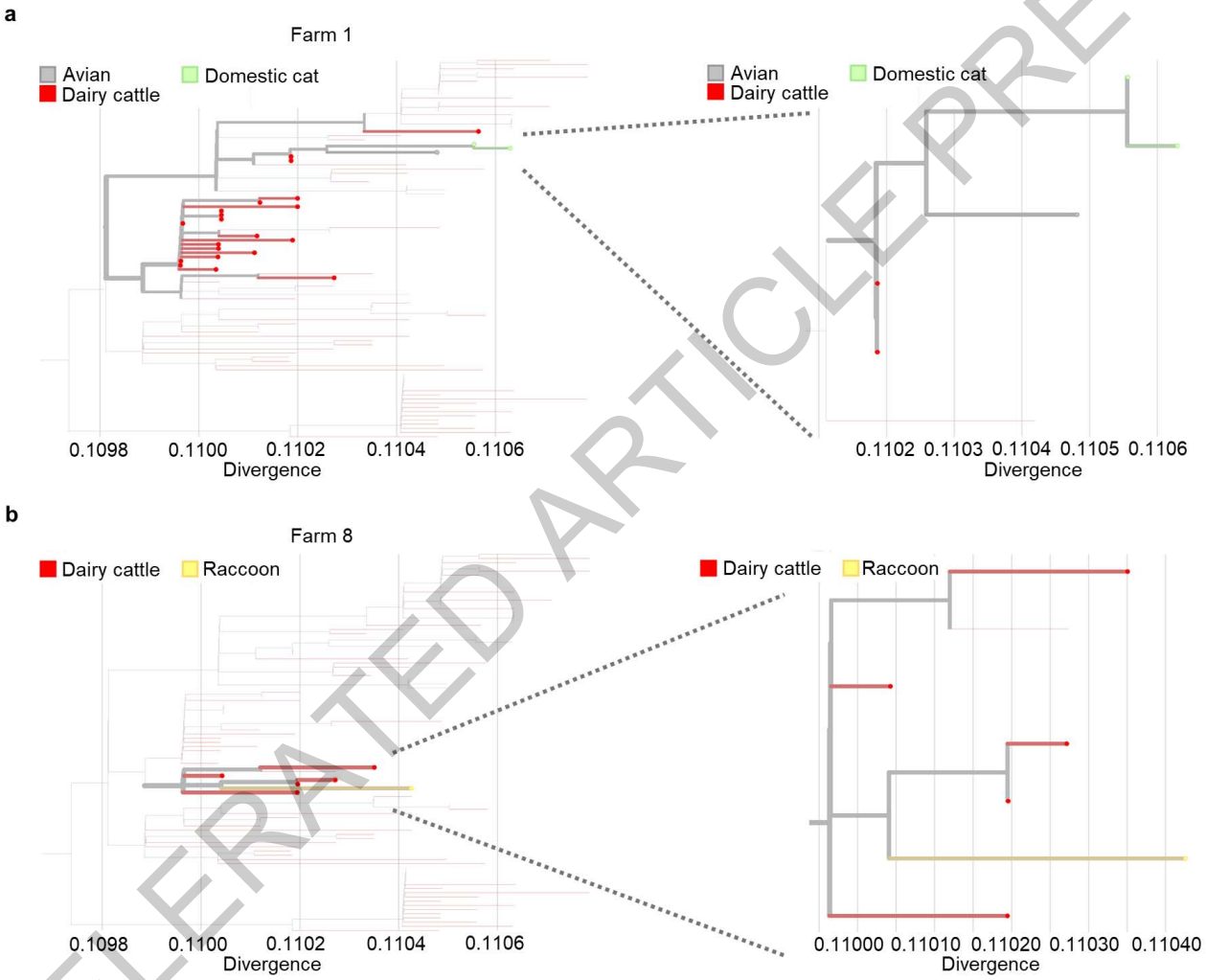

Extended Data Fig. 8

	Farm								
	1 (TX1)	**2 (TX2)**	**3 (OH1)**	**4 (NM1)**	**5 (TX3)**	**6 (TX4)**	**7 (TX5)**	**8 (NM2)**	**9 (KS1)**
Total number of dairy cows	4,000	35,000	3,350	4,200	7,000	4,000	6,600	4,000	10,000
Clinically affected cows[a]	800 (20%)	1,200 (3.42%)	787 (23.49%)	420 (10%)	1,400 (20%)	800 (20%)	528 (8%)	200 (5%)	1,000 (10%)
Clinical disease onset	03/09/24	02/11/24	03/21/24	03/17/24	03/08/24	03/10/24	03/14/24	03/15/24	03/19/24
Last clinical case recorded	04/03/24	Not available	04/13/24	03/30/2024	03/18/2024	03/29/2024	03/30/2024	03/25/2024	04/02/2024
Sample collection	03/13/24	03/13/24	03/29/24	03/20/24	03/14/24	03/10/24	03/15/24	03/16/24	03/25/24
HPAI virus was first detected	03/20/24	03/25/24	03/29/24	03/22/24	03/25/24	03/25/24	04/01/24	03/27/24	03/28/24
Other species affected	Grackles, pigeons, cats	-	Cats	Cats	Cats	-	-	Wild birds, cats, racoon	-
Clinical signs	Reduced feed intake, depression, anorexia, moderate dehydration, respiratory distress, clear nasal discharge, dry/tacky feces, milk with yellowish color, abrupt decrease in milk production (20-100% in individual affected animals). Dead cats (n=24), grackles and pigeons in the farm. Complete blood work on 10 cattle revealed mild hyperproteinemia and neutropenia.	Increased respiratory signs, pneumonia, decreased milk production, increased somatic cell count, increased mortality (>100 animals in 3 weeks). Large animal chemistry panels on 10 cows were consistent with anorexia and inflammation.	Reduced feed intake, reduced rumination, anorexia, dehydration, respiratory distress, nasal discharge, increased mortality, milk with yellow color, decreased milk production (20-100% in individual affected animals), increased somatic cell count. Increased mortality in dairy cattle in April (from average 50 per month to 99 during the clinical outbreak). Dead cats (n=6) in the farm.	Mastitis, change in milk consistency, constipation, diarrhea, pneumonia, decreased milk production. Most cows were in lactation 2 or greater.	Reduced feed intake and rumination, decreased milk production, abnormal fecal consistencies ranging from firm to soft, decreased capillary refill time. Most cows were in lactation 2 or greater.	Loose fecal material, decreased milk production, decreased food intake, yellow thickened milk, increased somatic cell count.	Decreased milk production, diarrhea, dehydration, mastitis, increased respiratory rate and lung sounds, fever.	Decreased milk production, increased respiratory rate, yellow creamy milk. Most cows were in lactation 2 or greater.	Decreased milk production, yellow creamy milk, tacky manure, poor rumen motility.

Extended Data Table 1

Clinical animals					Non-clinical animals				
Animal ID	**Milk**	**Nasal swab**	**Urine**	**Feces**	**Animal ID**	**Milk**	**Nasal swab**	**Urine**	**Feces**
1	22.39	NEG	-	-	26	-	NEG	NEG	NEG
2	9.67	NEG	-	-	27	NEG	37.37	-	-
3	29.97	NEG	NEG	NEG	28	NEG	27.51	-	-
4	24.54	NEG	-	NEG	29	-	NEG	-	NEG
5	14.39	33.69	-	-	30	NEG	37.31	NEG	NEG
6	28.03	36.57	NEG	NEG	31	NEG	NEG	-	-
7	24.61	NEG	NEG	NEG	32	NEG	NEG	-	-
8	17.40	NEG	-	-	33	NEG	38.93	26.57	NEG
9	32.75	38.52	NEG		34	NEG	NEG	-	-
10	25.31	NEG	NEG	NEG	35	NEG	37.52	-	-
11	31.78	NEG	NEG	NEG	36	NEG	NEG	-	-
12	14.82	NEG	-	-	37	NEG	NEG	-	-
13	32.73	NEG	NEG	NEG	38	NEG	NEG	-	-
14	0.00	NEG	32.44	NEG	39	-	-	36.45	NEG
15	26.39	NEG	30.41	NEG	40	NEG	NEG	-	NEG
16	21.30	NEG	-	-	41	NEG	NEG	26.02	NEG
17	32.60	NEG	NEG	NEG	42	29.45	36.60	30.86	NEG
18	28.74	NEG	NEG	NEG	43	-	NEG	NEG	NEG
19	30.79	35.36	NEG	NEG	44	-	NEG	NEG	NEG
20	34.16	NEG	NEG	NEG	45	NEG	NEG	-	-
21	33.20	NEG	NEG	NEG					
22	21.11	NEG	-	-					
23	33.42	39.82	-	-					
24	22.78	NEG	NEG	NEG					
25	12.13	32.94	-	-					

Extended Data Table 2

Tissues	Cattle				Cat	Viral RNA and antigen detection
	A240740398	A240750066	240830001	240750100	062222-24	
Mammary gland	+	N/T	+++	-	N/T	Epithelial cells of alveolar lumen.
Supra-mammary lymph node	+	++	-	N/T	N/T	Reticular epithelial cells of lymphoid follicles.
Ovary	N/T	N/T	N/T	N/T	+	Unidentified cells within corpus luteum.
Brain	-	-	N/T	N/T	+++	Neurons, glial cells, Purkinje cells, vascular endothelial cells, endothelial cells of choroid plexus.
Trachea	-	-	-	+	-	Subepithelial connective tissue.
Lung	+	-	-	N/T	++	BALT, bronchiolar epithelial cells, type II pneumocytes.
Heart	++	+	+	N/T	-	Endothelial cells of blood vessels and cardiomyocytes
Liver	+	+	-	-	+++	Resident sinusoidal Kupffer cells.
Spleen	+	+	+	-	+	Mononuclear cells
Tongue	-	-	-	N/T	N/T	-
Rumen	-	-	-	N/T	N/T	-
Reticulum	-	-	-	N/T	N/T	-
Omasum	-	-	-	N/T	N/T	-
Abomasum	-	-	-	N/T	N/T	-
Omentum	-	-	N/T	N/T	N/T	-
Small intestine	-	-	-	N/T	-	-
Colon	+	+	-	-	-	Goblet cells, GALT lymphocytes, vascular endothelial cells of serosa.
Kidney	-	-	-	N/T	-	-
Urinary bladder	-	-	-	N/T	N/T	-
Adrenal gland	-	-	-	N/T	N/T	-
Pancreas	-	-	-	N/T	-	-
Thyroid	-	-	-	N/T	N/T	-

Extended Data Table 3

Isolate	Collection date	Country/State	Genotype	PA	HA	NA	M	NS	PB2	PB1	NP
Mallard[A]	08/26/2021	Canada/AL	N/A (H11N9)	am1	--	--	--	--	am21	--	am8
Mallard[B]	11/08/2021	USA/New York	N/A (H5N4)	--	--	am1N4	--	am1.2	am5	am4	--
Chicken[C]	12/21/2021	Canada/NF	N/A (H5N1)	ea1	ea2	ea1	ea1	ea1	ea1	ea2	ea1
Wigeon[D]	12/30/2021	South Carolina	A1	ea1	ea1	ea1	ea1	ea1	ea1	ea1	ea1
Chicken[E]	06/15/2022	Canada BC	B3.2	ea1	ea1	ea1	ea1	am1.1	am2.1	am1.2	am1.4.1
Mallard[F]	08/22/2022	Canada AL	NA (H3N8)	--	--	--	--	am1.2	am2.2	am1.3	am1.1
Skunk[G]	11/04/2022	Idaho	B3.2	ea1	ea1	ea1	ea1	am1.1	am2.1	am1.2	am1.4.1
Skunk[H]	01/27/2023	Kansas	B3.2	ea1	ea1	ea1	ea1	am1.1	am2.1	am1.2	am1.4.1
Turkey[I]	11/20/2023	Minnesota	B3.6	ea1	ea1	ea1	ea1	am1.1	am18	am4	am1.4.1
Snow goose[J]	11/27/2023	Tennessee	Minor51	ea1	ea1	ea1	am1	am1.1	am5	am7	am8
Tundra swan[K]	11/28/2023	Minnesota	B3.9	ea1	ea1	ea1	ea1	am1.1	am2.2	am4	am1.4.1
Ross goose[L]	12/20/2023	Kansas	B3.7	ea1	ea1	ea1	ea1	am1.1	am2.2	am4	am4
Unknown host			B3.13	ea1	ea1	ea1	ea1	am1.1	am2.2	am4	am8
Canada goose[M]	01/25/2024	Wyoming	B3.13	ea1	ea1	ea1	ea1	am1.1	am2.2	am4	am8
Falcon[N]	02/14/2024	California	B3.13	ea1	ea1	ea1	ea1	am1.1	am2.2	am4	am8
Skunk[O]	02/23/2024	New Mexico	B3.13	ea1	ea1	ea1	ea1	am1.1	am2.2	am4	am8
Grackle[P]	03/18/2024	Texas	B3.13	ea1	ea1	ea1	ea1	am1.1	am2.2	am4	am8
Cat[Q]	03/20/2024	New Mexico	B3.13	ea1	ea1	ea1	ea1	am1.1	am2.2	am4	am8
Cattle[R]	03/20/2024	Texas	B3.13	ea1	ea1	ea1	ea1	am1.1	am2.2	am4	am8
Human[S]	03/28/2024	Texas	B3.13	ea1	ea1	ea1	ea1	am1.1	am2.2	am4	am8

Extended Data Table 4

Extended Data Table 5. Comparative mutational spectrum of H5N1 clade 2.3.4.4b genotypes in different host species from 2021-2024.

Genes	2021 Canada	2021 USA	2022 USA				2023 USA				2024 USA								Cattle (all)	Cattle (variant)	Variant frequency within cattle sequences (n = 180)
	Mutations	American wigeon	Harbor Seals	Avian species	Skunk	Red Fox	Human	Skunk	Harbor Seals	Avian species	Goat	Canada goose	Falcon	Skunk	Human TX	Human MI	Grackle	Cat			
		A1	A2	Multiple genotypes	B1.3/ B3.2	Minor01	ND	B3.2	A2	Multiple genotypes	B3.6	B3.13									
PB2 (n = 12)	T58A	T	T	T/A^{Ck}	T	T	-	T	T	T	T	A	A	A	A	A	A	A	A	A	100 %
	V109I	V	V	V/I/F^{MS}	V	V	-	V	V	V	I	I	I	I	I	I	I	I	I	I	100 %
	V139I	V	V	V/I^{MS}	V	V	-	V	V	V/I^{MS}	I	I	I	I	I	I	I	I	I	I	100 %
	V255A	V	V	V/I^{MS}	V	V	-	V	V	V/I/L^{GHO}	V	V	V	V	V	V	V	V	V	A	1.66 %
	E362G	E	E	E	E	E	-	E	E	E	E	E	E	E	E	G	G	G	G	G	100 %
	D441N	D	D	D	D	D	-	D	D	D	D	D	D	D	N	N	N	N	N	N	100 %
	V495I	V	V	V/I^{MS}	V	V	-	V	V	V/I^{MS}	V	I	I	I	I	I	I	I	I	I	100 %
	E627K	E	K	E/K^{MS}	E/K	E/K	-	K	E	E/K^{MS}	E	E	E	E	K	E	E	E	E	E	0 %
	M631L	M	M	M/V^{G}	M	M	-	M	M	M	M	M	M	M	M	L	L	L	L	L	100
	I647V	I	I	I/M^{WD}	I	I	-	I	I	I	I	I	I	I	I	I	I	I	I	V	1.11 %
	V649I	V	V	V	V	V	-	V	V	V/I	V	I	I	I	I	I	I	I	I	I	100 %
	I676A	T	T	T	T	T	-	T	T	T/I^{RTH}	T	A	A	A	A	A	A	A	A	A	100 %
	E677G	E	E	E/A^{MS}	E	E	-	E	E	E	E	E	E	E	E	E	E	E	E	G	21.6 %
PB1 (n = 5)	E75D	E	E	E	E	E	-	E	D	E/D	D	D	D	D	D	D	D	D	D	D	100 %
	M171V	M	M	M/K^{Ph}	M	M	-	M	M	M/V/I^{MS}	V	V	V	V	V	V	V	V	V	V	100 %
	S384P	S	S	S	S	S	-	S	S	S/P^{ML}	S	S	S	S	S	S	S	S	S	P	10.50 %
	I392V	I	I	I/T^{Co}	I	I	-	I	I	I	I	I	I	I	V	I	I	I	I	I	0%
	R430K	R	R	R	R	R	-	K	R/K	R/K	K	K	K	K	K	K	K	K	K	K	100 %
	E581K	E	E	E/K^{WD}	E	E	-	E	E	E/VG^{MS}	E	E	E	E	E	K	E	E	E	E	0%
	A587P	A	A	A	A	A	-	A	A	A/S/P^{MS}	P	P	P	P	P	P	P	P	P	P	100 %
	A741V	S	A	A/S^{MS}	A	A/S*	-	A	A		A	A	A	A	A	V	A	A	A	A	0%
PA (n = 16)	I13V	I	I	I	I	I	I	I	I	I/V^{MS}	I	I	I	I	I	I	I	I	I	V	10 %
	G99E	G	G	G	G	G	G	G	G	G/R^{GP}	G	G	G	G	G	G	G	G	G	E	1.66 %
	K113R	K	K	K	K	K	K	K	K	K/R^{MS}	R	R	R	R	R	R	R	R	R	R	100
	K142E	K	K	K/R*	K	K	K	K	K	K	K	K	E	E	E	K	K	K	K	K	0 %
	L219I	L	L	L	L	L	L	L	L	L	L	L	L	L	L	I	I	I	I	I	100 %
	R256K	R	R	R*	R	R	R	R	R	R	R	R	R	R	R	R	R	R	R	K	1.11 %
	K312R	K	K	K	K	K	K	K	K	K	K	K	K	K	K	K	K	K	K	R	2.22 %
	T357I	T	T	T/A^{Tk}	T	T	T	T	T	T	T	T	T	T	T	T	T	T	T	I	2.22 %
	M460I	M	M	T/A^{MS}	M	M	M	M	M	K	M	M	M	M/I	M	M	M	M	M	I	2.22 %
	K497R	K	K	K/R^{SG,GHO}	K	K	K	K	K	K	K	K	K	K	K	R	K	K	K	R	76 %
	E613K	E	E	E	E	E	E	E	E	E	E	E	E	E	E	E	E	E	E	K	11.1 %
	T143A	T	T	T	T	T	T	T	T	T/A^{PC}	T	T	T	T	T	T	T	T	T	A	5.55 %
	A172T	A	A	A	A	A	A	A	A	A/T^{WS}	A	A	A	A	A	A	A	A	A	T	3.88 %
HA (n =4)	T211I	T	T	T	T	T	T	T	T	T/I^{MS}	I	I	I	I	I	I	I	I	I	I	100 %
	S336N	S	S	S	S	S	S	S	S/N	S/N^{MS}	S	S	S	S	S	N	N	S	S	N	11.1 %
	E509G	E	E	E	E	E	E	E	E	E/G^{Tk}	E	E	E	E	E	E	E	E	E	G	2.22 %
	I546S	I	I	I	I	I	I	I	I	I	I	I	I	I	I	I	I	I	I	S	2.77 %
NA (n = 7)	V67I	V	V	V	V	V	V	V	V	V/I^{MS}	V	I	I	I	I	I	I	I	I	I	100 %
	N71S	N	N	N	N	N	N	N	N	Y^{BV}	N	N	N	N	N	N	N	N	N	S	10 %
	A232V	A	A	A/V^{Ck}	A	A	A	A	A	A/V^{MS}	A	A	V	A	A	A	A	A	A	V	1.11 %
	L269M	L	L	L	L	L	L	L	L	L/M^{MS}	L	M	M	M	M	M	M	M	M	M	100 %
	V321I	V	V	V	V	V	-	V	V	V/I^{MS}	I	I	I	I	I	I	I	I	I	I	100 %
	S339P	S	S	S	S	S	-	S	S	S/P^{MS}	P	P	P	P	P	P	P	P	P	P	100 %
	G454D	G	G	G/D^{BV}	G	G	-	G	G/S	G/D^{SG,Ck}	G	G	G	G	G	G	G	G	G	D	1.11 %
NP (n = 2)	G5S	G	G	G	G	G	-	G	G	G	G	G	G	G	G	G	G	G	G	S	1.11 %
	S482N	S	S	S	S	S	-	S	S/N	S/N^{Tk}	S	N	N	N	N	N	N	N	N	N	100 %
NS1 (n = 10)	S7L	S	S	S	S	S	-	S	S	S	S	S	S	S	L	L	L	L	L	L	100 %
	R21Q	R	R	R	R	R	-	R	R	R/Q^{CR}	S	R	R	R	R		R	R	R	Q	1.11 %
	T76A	T	T	T/A^{MS}	A	T/A^{MS}	-	A	A	T/A^{MS}	A	A	A	A	A	A	A	A	A	T	1.11 %
	L77R	L	L	L	L	L	-	L	L	L/P^{RH}	L	L	L	L	L	L	L	L	L	R	8.8 %
	A86T	A	A	A/T/D*	A	A	-	A	A	A/V/S	A	A	A	A	A	A	A	A	A	T	2.22 %
	C116S	C	C	C	C	C	-	C	C	C/S	S	S	S	S	S	S	S	S	S	S	100 %
	M124VT	M	M	M	M	M	-	M	M	M/V^{TV}	M	M	M	M	M	M	M	M	M	V/T	1.11 %
	D125N	D	D	D	D	D	-	D	D/N	D/N^{HLV}	D	D	D	D	D	D	D	D	D	N	12.22 %
	P212L	P	P	P	P	P	-	P	P	P/L^{RTH}	P	P	P	P	P	P	P	P	P	L	1.11 %
	E229K	E	E	E	E	E	-	E	E	E/K^{SG}	E	E	E	E	E	E	E	E	E	K	8.88 %

Note: A/chicken/NL/FAV-0033/2021|2021-12-21|2.3.4.4b was used as reference [first sequence detected in North America (Canada)]. -; gene fragment not available. All sequences used in the analysis are provided in supplementary data table 4. All the cattle HPAI H5N1 genotype B3.13 variants with <1% frequency are shown in the supplementary data table 6.
The superscripts are abbreviation of species; BV: black vulture, CG: Canada goose, Ck: chicken, Co: cormorant, CR: crow, E: eagle, ER: eared grebe, F: falcon, G: goose, GHO: great horn own, PC: peacock, RTH: red tail hawk, SG: snow goose, Tk: turkey, TV: turkey vulture, WD: wood duck, WS: western screech, MS: multiple species, Ph: pheasant, *: polymorphism, TX; Texas, MI: Michigan.
Highlighted rows colors; Light blue: mutation specific to HPAI H5N1 Clade 2.3.4.4b genotype B3.13, Pink: cattle variants with frequency above 5%, Green: mutations emerged in 2023 and circulated in cattle sequences in 2024, Brown: mutations in Human or human, falcon, and skunk sequences in 2024, Grey: virus adaptation mutation to mammalian hosts.

Extended Data Table 5

Tissues	Cattle				Cat	Microscopic changes
	A240740398	A240750066	240830001	240750100	062222-24	
Mammary gland	+	+	+	+	N/T	Neutrophilic and lymphoplasmacytic mastitis with significant effacement of tubuloacinar gland architecture filled with neutrophils admixed with cellular debris in multiple lobules of mammary gland.
Mammary gland lymph node	+	+	+	+	N/T	Lymphadenitis with 40-85% effacement of cortical. architecture by parafollicular hyperplasia in mammary gland lymph node.
Ovary	N/T	N/T	N/T	N/T	+	Non-significant non-specific microscopic changes.
Brain	+	+	+	N/T	+	Vascular congestion, mild perivascular hemorrhage, perivascular cuffing, mild gliosis, and meningeal vascular congestion in cattle brain. Mild to moderate multi-focal lymphohistiocytic meningoencephalitis with multifocal areas of parenchymal and neuronal necrosis in cat brain.
Trachea	N/T	N/T	N/T	+	N/T	Lymphoplasmacytic laryngitis with hyperplastic epithelium.
Lung	+	+	+	+	+	Lymphoplasmacytic interstitial pneumonia with. hypercellularity of alveolar septa expanded by a combination of fibrin in lungs.
Heart	-	-	-	N/T	-	Non-significant non-specific microscopic changes.
Liver	+	+	+	+	+	Mild lymphoplasmacytic hepatitis with single cell necrosis and focal telangiectasia in liver.
Spleen	-	-	-	-	+	Non-significant non-specific microscopic changes.
Tongue	-	-	-	N/T	N/T	Non-significant non-specific microscopic changes.
Rumen	-	-	-	N/T	N/T	Non-significant non-specific microscopic changes.
Reticulum	-	-	-	N/T	N/T	Non-significant non-specific microscopic changes.
Omasum	-	-	-	N/T	N/T	Non-significant non-specific microscopic changes.
Abomasum	-	-	-	N/T	N/T	Non-significant non-specific microscopic changes.
Omentum	-	-	N/T	N/T	N/T	Non-significant non-specific microscopic changes.
Small intestine	+	+	+	N/T	-	Segmental apical necrosis with blunting and fusion of villi in small intestine.
Colon	+	+	+	+	-	Mild neutrophilic and lymphoplasmacytic colitis with epithelial erosions in colon.
Kidney	-	-	-	N/T	-	Non-significant non-specific microscopic changes.
Urinary bladder	-	-	-	N/T	N/T	Non-significant non-specific microscopic changes.
Adrenal gland	-	-	-	N/T	N/T	Non-significant non-specific microscopic changes.
Pancreas	-	-	-	N/T	-	Non-significant non-specific microscopic changes.
Thyroid	-	-	-	N/T	N/T	Non-significant non-specific microscopic changes.

Extended Data Table 6

nature portfolio

Corresponding author(s): Diego G. Diel

Last updated by author(s): Jul 9, 2024

Reporting Summary

Nature Portfolio wishes to improve the reproducibility of the work that we publish. This form provides structure for consistency and transparency in reporting. For further information on Nature Portfolio policies, see our Editorial Policies and the Editorial Policy Checklist.

Statistics

For all statistical analyses, confirm that the following items are present in the figure legend, table legend, main text, or Methods section.

n/a	Confirmed	
☐	☒	The exact sample size (*n*) for each experimental group/condition, given as a discrete number and unit of measurement
☐	☒	A statement on whether measurements were taken from distinct samples or whether the same sample was measured repeatedly
☒	☐	The statistical test(s) used AND whether they are one- or two-sided *Only common tests should be described solely by name; describe more complex techniques in the Methods section.*
☒	☐	A description of all covariates tested
☒	☐	A description of any assumptions or corrections, such as tests of normality and adjustment for multiple comparisons
☐	☒	A full description of the statistical parameters including central tendency (e.g. means) or other basic estimates (e.g. regression coefficient) AND variation (e.g. standard deviation) or associated estimates of uncertainty (e.g. confidence intervals)
☒	☐	For null hypothesis testing, the test statistic (e.g. *F*, *t*, *r*) with confidence intervals, effect sizes, degrees of freedom and *P* value noted *Give P values as exact values whenever suitable.*
☐	☒	For Bayesian analysis, information on the choice of priors and Markov chain Monte Carlo settings
☒	☐	For hierarchical and complex designs, identification of the appropriate level for tests and full reporting of outcomes
☒	☐	Estimates of effect sizes (e.g. Cohen's *d*, Pearson's *r*), indicating how they were calculated

Our web collection on statistics for biologists contains articles on many of the points above.

Software and code

Policy information about availability of computer code

Data collection	No software was used for data collection.
Data analysis	1. GenoFlu tool (https://github.com/USDA-VS/GenoFLU) was used to identify the lineage of gene and genotyp e of H5N1 genome sequences. 2. GraphPad Prism software (v10) was used to perform statistical analysis and creation of graphical presentations of data. 3. Genious Prime software (v2024.0) was used to create local customized BLAST datasets and phylogenetic evolutionary analysis of individual genes of H5N1 genome sequences. 4. BEAST software (v1.10.1) was used to perform the time for most recent ancestral (tMRCA or MRCA) analysis. 5.Biorender (https://app.biorender.com/) was used to create the customized and create figure panels. 6. Nanofilt v2.8.0 (https://github.com/wdecoster/nanofilt/releases) was used to filter sequencing reads. 7. Kraken v2.1.0 (https://github.com/DerrickWood/kraken2) was used for taxonomic classification of sequencing reads. 8. Bracken v2.9 (https://github.com/jenniferlu717/Bracken) was used to estimate the abundance of each taxon in the sample. 9. Minialign v0.4.4 (https://github.com/ocxtal/minialign) was used for aligning reads to reference genome. 10. Medaka v1.4.3 (https://github.com/nanoporetech/medaka) was used for variant calling and consensus sequence polishing. 11. Trimmomatic v0.39 (https://github.com/timflutre/trimmomatic) was used to filter Illumina sequencing reads. 12. Snippy v4.6.0 (https://github.com/tseemann/snippy) was used for aligning, calling variants and generating consensus sequences of Illumina sequencing data. 13. Prokka v1.14.5 (https://github.com/tseemann/prokka?tab=readme-ov-file) was used to annotate genome sequences and identify genetic features and functional elements. 14. FluSurver tool v1 (https://flusurver.bii.a-star.edu.sg/) was used to interpret the effects of mutations identified in the sequences. 15. Nextstrain (https://github.com/nextstrain/avian-flu) was used for phylogenomic and phylogeographic analysis.

16. Auspice 0.12.0 (https://github.com/nextstrain/auspice) was used for interactive exploration of Nextstrain dataset.
17. PopART v1.7.2 (https://popart.maths.otago.ac.nz/) was used for haplotype network construction.
18. Augur v21.0.1 (https://github.com/nextstrain/augur) was used for phylogenomic analysis
19. MAFFT v7.515 (https://github.com/GSLBiotech/mafft) was used for multiple seuqence alignment.
20. IQ-TREE v1.6.12 (https://github.com/Cibiv/IQ-TREE) was used for phylogenetic tree construction.
21. TreeTime v0.9.4 (https://github.com/neherlab/treetime) was used for maximum likelihood dating and ancestral sequence inference.
22. TreeSort v.0.1.1 (https://github.com/flu-crew/TreeSort) was used for reassortment event inference.
23. FigTree v1.4.4 (http://tree.bio.ed.ac.uk/software/figtree/) was used for visualization of phylogenetic trees.
24. TreeAnnotator v1.8.4 (https://www.beast2.org/treeannotator/) was used to generate maximum clade credibility tree.
25. BEAGLE library v4.0.1 (https://github.com/beagle-dev/beagle-lib) was used to perform core calculations in BEAST software.

For manuscripts utilizing custom algorithms or software that are central to the research but not yet described in published literature, software must be made available to editors and reviewers. We strongly encourage code deposition in a community repository (e.g. GitHub). See the Nature Portfolio guidelines for submitting code & software for further information.

Data

Policy information about availability of data

All manuscripts must include a data availability statement. This statement should provide the following information, where applicable:

- Accession codes, unique identifiers, or web links for publicly available datasets
- A description of any restrictions on data availability
- For clinical datasets or third party data, please ensure that the statement adheres to our policy

All HPAI H5N1 virus sequences generated in this study are deposited in GISAID (https:www.gisaid.org/; accession numbers are available in Supplementary Data Table 5), and raw reads have been deposited in NCBI's Short Read Archive (BioProject number PRJNA1114404). All additional influenza sequences used in our analysis were obtained from GISAID (accession numbers available in Supplementary Data Table 4), or NCBI nucleotide (https://www.ncbi.nlm.nih.gov/nucleotide/).

Research involving human participants, their data, or biological material

Policy information about studies with human participants or human data. See also policy information about sex, gender (identity/presentation), and sexual orientation and race, ethnicity and racism.

Reporting on sex and gender	n/a
Reporting on race, ethnicity, or other socially relevant groupings	n/a
Population characteristics	n/a
Recruitment	n/a
Ethics oversight	n/a

Note that full information on the approval of the study protocol must also be provided in the manuscript.

Field-specific reporting

Please select the one below that is the best fit for your research. If you are not sure, read the appropriate sections before making your selection.

☐ Life sciences ☐ Behavioural & social sciences ☒ Ecological, evolutionary & environmental sciences

For a reference copy of the document with all sections, see nature.com/documents/nr-reporting-summary-flat.pdf

Ecological, evolutionary & environmental sciences study design

All studies must disclose on these points even when the disclosure is negative.

Study description	This study consisted of a diagnostic and epidemiological investigation conducted in dairy farms in the US experiencing an a clinical outbreak of sudden milk drop and respiratory distress. Clinical samples were collected by field veterinarians and submitted to three veterinary diagnostic laboratories for testing. Genomic surveillance was conducted, identifying, highly pathogenic avian influenza (HPAI) H5N1 infection in cattle. Epidemiological data collected from the farms was combined with genomic sequence data to make inferrences from virus transfer and transmission pathways between affected farms.
Research sample	Nine dairy farms (Farms 1-9) were included in our study. These farms all experienced a clinical outbreak with sudden drop in milk production and respiratory distress which was confirmed to be caused by HPAI H5N1. A total of 332 samples collected from dairy cattle (n=323), domestic cats (n=4), great-tailed grackles (n=3), pigeon (n=1) and a racoon (n=1) in the affected farms were submitted for the initial diagnostic investigation. Follow up samples were collected and submitted by Farm 3. These included sequential samples (milk, nasal swabs and blood)

	collected from animals (n=15) which were used to investigate duration of virus shedding. Additionally, paired samples (milk, nasal swabs, urine and feces) collected from animals presenting respiratory distress, drop in milk production and altered milk characteristics (clinical, n=25) and from apparently healthy animals (non-clinical, n=20) from Farm 3 were used to compare virus shedding by clinical and non-clinical animals
Sampling strategy	Because this was a clinical disease outbreak of unknown etiology, mostly samples from clinically affected animals were collected initially. To determine duration of virus shedding sequential samples were collected from clinically affected animals. Additionally, to investigate infection and shedding of virus by sub-clinical animals samples from clinical and nonclincial dairy cows from. Samples from other species, including birds, cats and raccoons were sent to the diagnostic laboratories for diagnostic investigation due to mortality outbreaks in these species.
Data collection	clinical sample data was collected and generated by diagnostic laboratories involved in the investigation. Epidemiological information from farms was collected via official sample submission forms provided by the farm veterinarians or follow up epidemiological investigations with the field/farm veterinarians. Sequencing data were generated in each of the participating diagnostic laboratories. Additional sequences that were collected and tested from the Farms in our study were obtained from GISAID.
Timing and spatial scale	Sample collection timeline: 03/10/24 to 04/02/2024.
Data exclusions	Clinical samples that did not generate complete HPAI H5N1 genomes were not included in the analysis.
Reproducibility	Clinical samples were tested by RT-PCR following standard operating procedures established at the National Animal Health Laboratory Network. Confirmatory testing of the initial submissions from each farm was performed at the National Veterinary Services Laboratories.
Randomization	Not relevant for this study, as it consisted of a diagnostic investigation.
Blinding	No blinding was applied in the study. Samples were tested as routine diagnostic samples in the testing laboratories.

Did the study involve field work? ☒ Yes ☐ No

Field work, collection and transport

Field conditions	Not known. Samples were submitted by farm veterinarians. Samples were submitted to the testing laboratories on ice packs and maintained refrigerated until tested.
Location	TX, NM, KS and OH
Access & import/export	Not applicable.
Disturbance	Not applicable.

Reporting for specific materials, systems and methods

We require information from authors about some types of materials, experimental systems and methods used in many studies. Here, indicate whether each material, system or method listed is relevant to your study. If you are not sure if a list item applies to your research, read the appropriate section before selecting a response.

Materials & experimental systems

n/a	Involved in the study
☐	☒ Antibodies
☐	☒ Eukaryotic cell lines
☒	☐ Palaeontology and archaeology
☒	☐ Animals and other organisms
☒	☐ Clinical data
☒	☐ Dual use research of concern
☒	☐ Plants

Methods

n/a	Involved in the study
☒	☐ ChIP-seq
☒	☐ Flow cytometry
☒	☐ MRI-based neuroimaging

Antibodies

Antibodies used	Anti-nucleoprotein mouse monoclonal antibody (HB65, ATCC, H16-L10-4R5); monoclonal antibody (Meridian Bioscience, Catalog No. C65331M) to Influenza A virus M-gene
Validation	Positive and negative controls were used in all the tests performed with these antibodies.

Eukaryotic cell lines

Policy information about cell lines and Sex and Gender in Research

Cell line source(s)	bovine uterine epithelial cells (CAL-1; bovine, female)
Authentication	cell was not authenticated using genomic methods, but is highly susceptible to several bovine viruses including bovine viral diarrhea virus, bovine herpesvirus 1, bovine adenovirus, etc.
Mycoplasma contamination	CAL-1 cells are tested routinely twice a year for mycoplasma and tested negative.
Commonly misidentified lines (See ICLAC register)	n/a

Plants

Seed stocks	n/a
Novel plant genotypes	n/a
Authentication	n/a